

“EVALUATION OF AMIP-TYPE ATMOSPHERIC FIELDS AS FORCING FOR MEDITERRANEAN SEA AND GLOBAL OCEAN REANALYSES”

Annalisa Cherchi^{1,2,*}, Satyaban Bishoyi Ratna³, Simona Masina^{1,2}, Andrea Storto¹, Chunxue Yang⁴, Claudia Fratianni², Simona Simoncelli², Nadia Pinardi⁵

⁽¹⁾ Fondazione Centro Euro-Mediterraneo sui Cambiamenti Climatici, Bologna, Italy

⁽²⁾ Istituto Nazionale di Geofisica e Vulcanologia, Bologna, Italy

⁽³⁾ Climatic Research Unit, School of Environmental Sciences, University of East Anglia, Norwich, United Kingdom

⁽⁴⁾ Institute of Marine Sciences, National Research Council (ISMAR-CNR), Roma, Italy

⁽⁵⁾ Università degli Studi di Bologna, Bologna, Italy

Article history

Received June 1, 2018; accepted November 7, 2018.

Subject classification:

Ocean reanalyses; AMIP experiments; Atmospheric forcing; Mediterranean Sea; Global ocean.

ABSTRACT

Oceanic reanalyses are powerful products to reconstruct the historical 3D-state of the ocean and related circulation. At present a challenge is to have oceanic reanalyses covering the whole 20th century. This study describes the exercise of comparing available datasets to force Mediterranean Sea and global oceanic reanalyses from 1901 to present. In particular, we compared available atmospheric reanalyses with a set of experiments performed with an atmospheric general circulation model where sea surface temperature (SST) and sea-ice concentration are prescribed. These types of experiments have the advantage of covering long time records, at least for the period for which global SST is available, and they can be performed at relatively high horizontal resolutions, a very important requisite for regional oceanic reanalyses. However, they are limited by the intrinsic model biases in representing the mean atmospheric state and its variability. In this study, we show that, within some limits, the atmospheric model performance in representing the basic variables needed for the bulk-formulae to force oceanic data assimilation systems can be comparable to the differences among available atmospheric reanalyses. In the case of the Mediterranean Sea the high horizontal resolution of the set of SST-prescribed experiments combined with their good performance in representing the surface winds in the area made them the most appropriate atmospheric forcing. On the other hand, in the case of the global ocean, atmospheric reanalyses have been proven to be still preferable due to the better representation of spatial and temporal variability of surface winds and radiative fluxes. Because of their intrinsic limitations AMIP experiments cannot provide atmospheric fields alternative to atmospheric reanalyses. Nevertheless, here we show how in the specific case of the Mediterranean Sea, they can be of use, if not preferable, to available atmospheric reanalyses.

1. INTRODUCTION

Oceanic reanalyses over multi-decadal periods are powerful instruments to reconstruct the 3D-state of the ocean and the large-scale circulation over the recent past. Outputs are specifically useful for the analysis of un-observed quantities, such as meridional overturning circulation and oceanic fresh water and heat transports

[Masina et al., 2011]. An example of an important application is the initialization of coupled climate models with oceanic data assimilation products, as it has been found that they can improve both the seasonal [e.g. Balmaseda et al., 2009; Alessandri et al., 2010] and the decadal [Bellucci et al., 2013; Pohlmann et al., 2013] prediction skills. Recently, international efforts provided comparison and validation of different global oceanic

reanalyses [Masina et al., 2017].

Atmospheric fluxes (momentum, heat and freshwater) needed for oceanic reanalyses can be derived using bulk-formulae and they are usually taken from atmospheric reanalysis products, such as NCEP/NCAR [Kalnay et al., 1996], ERA40 [Uppala et al., 2005], JRA-25 [Onogi et al., 2005] and ERA-Interim [Dee et al., 2011]. These products assimilate meteorological observations into numerical weather prediction (NWP) models. Atmospheric reanalysis products share similar physical assumptions and they assimilate common observations, but different physical parameterizations and different assimilation techniques or quality control procedures can yield different results. Sometimes corrections are applied to the original atmospheric reanalyses adjusting them to available satellite-based and in-situ derived data [i.e. Large and Yeager, 2004; Brodeau et al., 2010; Pettenuzzo et al., 2010; Dussin and Barnier, 2013]. However, comparing available atmospheric reanalyses, it is hard to conclude with one product that agrees best with satellite-derived observations [Chaudhuri et al., 2013].

In this study we describe the exercise of looking for a suitable atmospheric forcing dataset to produce ocean reanalyses over the Mediterranean Sea and the global ocean for the whole 20th century. In regional oceanic reanalysis's applications, atmospheric forcing fields need two important characteristics: relatively high spatial and temporal resolution and passing surface winds. In the Mediterranean Sea the assessment of surface winds forcing is a pre-requisite to obtain realistic characterization of the basin circulation [Demirov and Pinardi, 2002; Korrer et al., 2000].

Because of the need to assimilate available observations with the largest coverage possible, most of the atmospheric reanalyses cover the last few decades. However, (proxy) observations of SST and of surface pressure are available back to at least the beginning of the 20th century. In fact, atmospheric reanalyses covering the whole century using only surface pressure and SST are now available. For example, the Twentieth Century Reanalysis [20CRv2; Compo et al., 2011] assimilates only surface pressure and it uses reconstructed monthly sea surface temperature and sea-ice distributions as boundary conditions. This reanalysis in fact has already been used to force long global oceanic reanalyses [Yang and Giese, 2013; Yang et al., 2014]. Similarly, the European Center for Medium Range Weather Forecasts (ECMWF) has provided a 20th 80 Century reanalysis (ERA-20C) that assimilates only surface observations [Poli et al., 2013; Stickler et al., 2014], with the aim of repeating a similar exercise to that of Compo et al. [2011], in order to evaluate the feasibility of centennial atmospheric reanalyses.

These long atmospheric reanalyses assimilate only surface fields observations without taking information from upper air or remote sensors, with the aim of constructing a time-consistent reanalysis affected as little as possible by changes in observing networks. This implies however that the accuracy of such reanalyses is significantly lower than their full-observations counterparts [e.g. ERA-20C vs ERA-Interim, Poli et al., 2013].

At the time of this analysis, the only centennial atmospheric reanalysis available was 20CRv2. As it has been considered too coarse to be used for the Mediterranean Sea oceanic reanalysis we decided to explore an alternative forcing dataset, i.e. an ensemble of experiments performed with an Atmospheric General Circulation Model (AGCM) with prescribed interannually varying SST and sea-ice concentration as boundary conditions, identified as AMIP-type experiments. The acronym AMIP refers to the Atmospheric Model Intercomparison Project (AMIP) aimed at providing an ensemble of experiments with different AGCMs forced with the same boundary conditions [Gates, 1992]. AMIP-type experiments are important because they allow studying the way in which the atmosphere responds to the surface SST forcing in terms of heating and water fluxes [Rowntree, 1972, 1976]. However, they lack the feedback of atmosphere on ocean, hence they do not perform as well in the regions where atmospheric forcing plays an important role in inducing SST anomalies, such as the extra-tropics and tropical Indo-Western Pacific regions [i.e. Lau and Nath, 1994; Alexander et al., 2002; Krishnamurthy and Kirtman, 2003]. In the 1990s a variety of studies have shown that a single realization of a simulation is of limited use [Palmer, 1993; Stern and Miyakoda, 1995, among others], hence in climatological applications scientists started to provide a number of simulations with the same boundary conditions but different initial conditions (ensembles) to allow the natural instability of the system to generate different realizations of the climate variability.

Normally, reconstructed SST fields are able to ensure realistic interannual variability of atmospheric temperature, although their accuracy increases with time along with the increase on the number of available SST observations. In fact, the ensemble of AMIP experiments is able to reproduce the atmospheric warming for the whole 20th century, in agreement with contemporary reanalyses and reconstructions [Hersbach et al., 2015]. As the SST contains the signature of important dominant modes of variability, like El Niño Southern Oscillation (ENSO) and the Pacific Decadal Oscillation [PDO Mantua et al., 1997], AMIP experiments are useful to study

their forcing and associated teleconnections, including the potential predictability [Grassi et al., 2012; Cherchi and Navarra, 2013; Allen et al., 2014].

In this study, aware of the limitations described above, we explore whether AMIP-type experiments could represent a useful set of atmospheric variables to force oceanic reanalysis for the Mediterranean Sea primarily, and also for the global ocean. As far as we know this approach has never been tested before. The assessment of the atmospheric forcing from historical atmospheric reanalyses and AMIP experiments for global and regional long oceanic reanalysis is an important preliminary step before starting the reanalysis production itself. To do that we compare AMIP-type experiments and available atmospheric reanalyses in terms of the variables needed for the bulk-formulae to provide heat, water and momentum fluxes at the surface to the ocean general circulation model. In our comparison, the ERA-Interim reanalysis [Dee et al., 2011] is considered as a reference to evaluate the performance of AMIP-type experiments and other atmospheric reanalyses, as well as their usefulness in this framework. In fact, ERA-Interim is the product used to produce MyOcean global oceanic reanalyses [Masina et al., 2015] and the last Mediterranean Sea reanalysis covering the period 1987-2013 [Simoncelli et al., 2015].

The present study is organized as follows: Section 2 describes the datasets and the methodology used. It is organized into (i) AMIP experiments (Section 2.1), (ii) atmospheric reanalyses and other observations (Section 2.2) and (iii) the variables selected for the comparison and the methodology of the analysis (Section 2.3). Section 3 collects the main results of the study organized into comparisons between atmospheric reanalyses and AMIP-type experiments in terms of annual and seasonal mean climatologies for the Mediterranean Sea (Section 3.1) and the global ocean (Section 3.2). Some aspects of the interannual variability and linear trends for both Mediterranean Sea and global ocean are shown in Section 3.3. Finally, section 4 summarizes the main conclusions of the study.

2. DATA AND METHODOLOGY

2.1 AMIP-TYPE EXPERIMENTS

The set of AMIP-type experiments (AMIP) is performed with the ECHAM4 [Roeckner et al., 1996] AGCM at T106L19 (about 1.1°) resolution. Different initial conditions are applied to produce an ensemble of nine members, all sharing the same interannually varying SST and sea-ice concentration (SIC) taken

from HadISST1.1 [Rayner et al., 2003]. The nine AMIP members do not share the same length in time: five of them cover the period 1899-2010, while the other four have been executed for a shorter period (1930-2010). Concentrations of atmospheric CO_2 , ozone and other greenhouse gases are fixed to the values averaged for the 1990s. The whole ensemble has been validated for tropical variability and teleconnections in the South Asian monsoon region [Cherchi and Navarra, 2013; Cherchi et al., 2018] and in southeastern South America [Cherchi et al., 2014], mostly for the second half of the 20th century. In AMIP important coupling feedbacks like increased northward transport of heat by ocean currents or changes in infrared emission and increased absorbed solar radiation because of more open water associated with loss of sea-ice, are missing and they can be sources of important limitations in their potential use over Polar regions.

2.2 ATMOSPHERIC REANALYSES AND OBSERVATIONS

ERA-Interim is a reanalysis produced at ECMWF that covers the meteorological satellite era (1979-present). It implements a 4D-Var assimilation scheme capable of assimilating all in-situ meteorological observations, satellite radiance, GPS radio occultation data and satellite-derived wind vectors. It uses an adaptive bias correction scheme that avoids abrupt changes of the analyzed parameters when the observing networks change [Dee and Uppala, 2009]. The resolution is about 0.75° (T255) with 60 vertical levels. Lower boundary conditions are provided by different SST and sea-ice concentration analysis schemes throughout the reanalysis period [Dee et al., 2011]. The atmospheric greenhouse gases are assumed to be globally well mixed and are set to observed 1990 values plus a linear trend [Dee et al., 2011]. ERA-Interim assimilates QuickSCAT data but it is not visible in the spectral winds and it does not improve the reanalysis fields [Milliff et al., 2011].

ERA-Interim precipitation is used here after being corrected using the Global Precipitation Climatology Project (GPCP) dataset [Adler et al., 2003]. The corrected precipitation dataset (ERA-Interim) is the same used in the CMCC MyOcean global ocean reanalysis [Storto et al., 2016]. The correction is based on the application of a spatially varying monthly climatological coefficient, computed within the period 1989-2008 by comparing ERA-Interim and a satellite based passive microwave precipitation product [REMSS/PMWC, Hilburn and Wentz, 2008]. The correction is able to mitigate the overestimation of the ERA-Interim pre-

precipitation in tropical areas [Janowiak et al., 2010], thus significantly reducing the corresponding fresh water bias in ocean applications [Storto et al., 2012].

The 20CRv2 is a long atmospheric reanalysis, from 1871 to 2010, that uses an Ensemble Kalman Filter to assimilate surface pressure observations from the International Surface Pressure Databank (ISPD). The model resolution is about 2° (T62L28). Lower boundary conditions (SST and SIC) are provided by the Met Office HadISST1.1 [Rayner et al., 2003] dataset. The model configuration uses a time-varying definition of

operational forecasting system [Tonani et al., 2008; Oddo et al., 2009; Tonani et al., 2011]. CMAP is a technique which produces pentad and monthly analyses of global precipitation merging observations from rain gauges with estimates from several satellite-based algorithms (infrared and microwave). Analyses are available from 1979 to present in a global regular 2.5° spatial grid.

Gridded daily wind vectors, produced from the new QuikSCAT wind retrieval (i.e. QuikSCAT V3, <ftp://podaac.jpl.nasa.gov/OceanWinds/quikscat/pre->

Name	Type	Variables	Region	Period	Resolution	Reference
AMIP	AGCM exp	T2M, U10, V10, LWRD, SWRD, PRECIP, MSL, D2M, CLC	GLOB & MED	1901-2010	1.125°	Cherchi et al. [2014]
ERA-Interim	ECMWF reanalysis	T2M, U10, V10, LWRD, SWRD, PRECIP, MSL, D2M, CLC	GLOB & MED	1979-2010	0.75°	Dee et al. [2011]
20CRv2	NOAA reanalysis	T2M, U10, V10, LWRD, SWRD, PRECIP	GLOB	1901-2010	2°	Compo et al. [2011]
ERA40	ECMWF reanalysis	T2M, U10, V10, D2M, CLC	MED	1958-2001	1.125°	Uppala et al. [2005]
ERA-INC	Corrected ECMWF reanalysis	PRECIP	GLOB & MED	1979-2010	0.75°	Storto et al. [2012]
CMAP	Satellite & gauge data	PRECIP	MED	1979-2010	2.5°	Xie and Arkin [1997]
QuikSCAT	Satellite data	U10, V10	MED	2000-2003	0.25°	Bentamy and Croize-Fillon [2012]

TABLE 1. List of the datasets considered in the analysis with details of some characteristics, like: type of data, variables selected, region of analysis (GLOB for global ocean and MED for Mediterranean Sea), length of the data, spatial resolution and reference.

CO₂ and aerosol concentrations, and a prognostic ozone scheme. In 20CRv2 the treatment of the sea-ice concentration near the coastal areas induces a warm bias of the lower troposphere [Compo et al., 2011], largely visible in terms of temperature at 2 m and longwave and shortwave radiation at the surface. 20CRv2 has clear spectral signatures in surface wind components, evident as oscillations in long-term mean values [Kent et al., 2013].

Data from CPC Merged Analysis of Precipitation [CMAP; Xie and Arkin, 1997] is included in the comparison in section 3.1, as it represents the reference for precipitation in use for the Mediterranean Sea

view/L2B12/v3) are available from 2000 to 2003 with a spatial resolution of 0.25°. In the dataset, the computation of daily gridded wind fields from scatterometer wind observations is performed by means of the same objective method used for the estimation of daily ASCAT (DASCAT) wind fields [Bentamy and Croize-Fillon, 2012].

Table 1 summarizes all the datasets considered (reanalyses, observations and AMIP experiments), with some details like: spatial resolution, type of data, selected variables, region (i.e. global ocean or Mediterranean Sea) and period of analysis, and reference.

2.3 VARIABLES SELECTED AND METHODOLOGY

Because of the different bulk formulae needed to the data assimilation schemes used for the Mediterranean Sea [Pettenuzzo et al., 2010] and over the global ocean [Large and Yeager, 2009], the variables considered in the comparison are different. In particular, they are air temperature at 2 m (T2M), dew point temperature at 2 m (D2M), zonal and meridional wind components at 10 m (U10, V10), mean sea level pressure (MSL), total cloud cover (CLC) and total precipitation (PRECIP) for the Mediterranean Sea. Total precipitation is the sum of convective and large-scale liquid and solid precipitation. While they are T2M, specific humidity at 2 m (SH2), U10 and V10, downward longwave and shortwave radiative fluxes (LWRD and SWRD, respectively) and PRECIP for the global ocean.

The assessment of annual means (Section 3.1 and 3.2) is done in terms of differences and root mean squared error (RMSE). RMSE is computed taking the difference of annual means for the datasets of interest. For the Mediterranean Sea the longest AMIP members available (i.e. 5 out of 9) are used and compared. Annual and seasonal means of temperature, humidity, sea level pressure and cloud cover are based on the climatology of the period 1979–2001 (Figures 1,2,4). While precipitation is compared for the period 1979–2010 (Figure 3). Winds over the Mediterranean Sea are assessed also in comparison with QuikSCAT satellite data available from 2000 to 2003 (Figures 5,12). For all the variables, only sea-points in the Mediterranean basin (6°W–37°E, 30°–46°N) are considered in the analysis. Over the global ocean AMIP variables are taken as ensemble mean and they have been compared with ERA-Interim and 20CRv2 reanalyses. To be compared the fields are interpolated onto a common horizontal grid, and the coarsest (i.e. 2°) among them is chosen. Two periods of analysis are considered: 1979–2010, corresponding to the period in common between the three datasets, where all nine members are considered for the AMIP ensemble mean (Figures 6–10), and 1901–2010 where only the 5 longest members are considered for the ensemble mean (Figure 11). As the analysis is focused over the ocean, all the variables are masked over land-points.

The variability (Section 3.3) is analyzed in terms of standard deviations and correlation coefficients of monthly mean anomalies, removing the annual climatology (Table 2 and 3). All values are computed as averages over the Mediterranean Sea (MED) and over global ocean (GLOB). For standard deviations, the time period is 1979–2001 for MED values and 1979–2010 for GLOB values (Table 2). Instead in Table 3 the period of analysis depends on the length of the datasets considered and is specified in brackets.

3. RESULTS

3.1 COMPARISON OVER THE MEDITERRANEAN SEA

Figure 1 shows the annual cycle of T2M, D2M, MSL and CLC averaged over the Mediterranean basin for the common period (1979–2001) comparing AMIP with ERA40 and ERA-Interim. AMIP members tend to share the same seasonal cycle but they differ from reanalysis products (Figure 1). In particular, AMIP members tend to slightly overestimate T2M in boreal fall and winter (Figure 1a), while they slightly underestimate D2M in boreal summer (Figure 1b). The discrepancy in T2M seasonal cycle might be associated to the assimilation of SYNOP stations over land in both ECMWF reanalyses, spreading the land temperature analysis increments over sea [Simoncelli et al., 2011]. AMIP members have a MSL seasonal cycle wider than both ECMWF reanalyses (~14 hPa vs ~6 hPa), with larger climatological values from October to April and smaller ones from May to August (Figure 1c). For CLC the seasonal cycle of AMIP members differs from both reanalyses by about 5% and the differences are largest in boreal summer (Figure 1d). In boreal fall, winter and spring the differences between ERA40 and ERA-Interim may be ascribed to the substantial upgrades of microphysics, radiation and convection schemes from one atmospheric reanalysis to the other [Dee et al., 2011; Beljaars et al., 2006]. AMIP members tend to be closer to ERA-Interim, mostly in boreal winter and spring (Figure 1d).

Spatial maps of RMSE of AMIP T2M vs ERA-Interim and ERA40 reanalyses show generally small values in the Mediterranean basin (Figure 2). For AMIP vs ERA-Interim the largest values are located along the coasts (Figure 2a) with a maximum in the Northern Aegean Sea, close to the Dardanelles (for details of the geography of the Mediterranean Sea refer to Figure 5i). Instead for AMIP vs ERA40 the largest values are mostly in the Mid and Southern Adriatic (Figure 2b), where deep/intermediate water mass formation might happen [Pinardi et al., 2015; Simoncelli and Pinardi, 2018].

For PRECIP a comparison is done in terms of seasonal cycle of precipitation area-averaged in the Mediterranean Sea derived from AMIP members, ERA-Interim and CMAP, and in terms of RMSE of AMIP versus observations and reanalysis (Figure 3). The seasonal cycle of precipitation suggests consistency among ERA-Interim and AMIP members, with some differences in April, May and September when ERA-Interim precipitation is more intense (Figure 3a). CMAP presents a narrower seasonal cycle with less precipitation in November–December and more in April to September (Figure 3a, yellow line). ERA-Interim has been evaluated to give the correct water budget in the Mediterranean Sea reanalysis for recent decades [1987–2017; Si-

moncelli et al., 2016]. Both RMSE maps of precipitation (Figures 3b,c) exhibit the largest values in the Adriatic Sea and in the northeastern side of the basin (Figures 3b,c), reflecting the latitudinal gradient of precipitation in the Mediterranean Sea. The spatial RMSE pattern suggests a latitudinal shift of AMIP precipitation field (Figures 3b,c).

Figure 4 shows the seasonal cycle of meridional and zonal wind at 10 m, including the wind speed. AMIP meridional winds have large negative values indicating that AMIP northerly winds are more intense (Figure 4b), while the zonal component is comparable between the reanalyses and the AMIP members (Figure 4a). In terms of wind speed, AMIP monthly climatology has a wider seasonal cycle and the intensity is larger than both reanalyses from September to June, with ERA40 having the weakest wind (Figure 4c).

Winds are crucial in the Mediterranean Sea circulation for the basin energetics [Cessi et al., 2014]. Thus, the first concern is to get winds at appropriate magnitude in order to maintain the bulk of the circulation energy. The surface atmospheric wind (operationally defined at 10 meters from the surface) is directly used to derive surface stress and turbulent flux fields from bulk formulae. This implies that errors in the determination of the winds can alter the model forcing and have an impact on the output of the ocean circulation models [Myers et al., 1998].

To better validate AMIP and reanalyses products, we compare surface winds with satellite observations derived from QuikSCAT data. In order to compare the different datasets, AMIP and ECMWF reanalyses monthly mean data have been horizontally interpolated onto the QuikSCAT grid, masking land points over the whole Mediterranean basin. The comparison of wind speeds in terms of spatial patterns using the mean from 2000-2003 is shown in Figure 5. The regions with most intense winds shown from QuikSCAT observations (Figure 5a) are the Gulf of Lion to the east of Corsica, the Bonifacio Strait, the Sicily Strait, the sea regions east and west of Crete and the Aegean Sea (see Figure 5i for details of the geography of the Mediterranean 291 Sea). The winds spatial patterns reflect the two main wind regimes over the Mediterranean Sea: the strong and northwesterly Mistral, crossing the western Mediterranean, and the strong, dry northerly Etesian winds over the Aegean Sea. Wind speed is largely underestimated in both ERA40 and ERA-Interim (Figures 5b,c). On the other hand, AMIP members are able to reproduce both spatial patterns distribution and intensities (Figures 5d,h). Nevertheless, some features are not well captured by models' products. For example, neither reanalyses nor AMIP are able to reproduce the two maxima east and west of Crete, mostly associated with orographic forcing, as they all tend to have just one maximum (Figure 5).

3.2 COMPARISON OVER THE GLOBAL OCEAN

The comparison of temperature at 2 m in terms of the annual cycle shows that both AMIP and 20CRv2 are slightly warmer than ERA-Interim (Figures 6a,c). Globally, they are warmer by about 0.3° C for the whole year-climatology (Figure 6a). In the Northern Hemisphere, they are both warmer by about 0.5° C in boreal summer, while in boreal winter the bias in the 20CRv2 reanalysis is almost doubled compared to AMIP (Figure 6b). In the Northern Hemisphere the differences are smaller than in the Southern Hemisphere, but in both cases the largest discrepancies are found in local winters for 20CRv2 (Figure 6c). These biases are stronger in the polar regions where 20CRv2 is drastically warmer (more than 4°C) than ERA-Interim and AMIP (Figures 6d,e). In fact, the RMSE in the polar regions is the largest (Figure 6g) and it is associated with the winter hemisphere. Far from the poles, the differences in 20CRv2 are smaller than 1°C (Figure 6e), with the lowest value of RMSE apart for some coastal regions, like South America (Figure 6g). On the other hand, in AMIP the differences can reach 1.5° C, and far from the poles the largest values of RMSE are located in the western boundaries of the oceans (Figure 6f), mostly along the Gulf Stream and the Kuroshio currents. To have an idea on how the data sets differ in time, Figure 6h shows squared differences of monthly mean temperature averaged from 60°S to 60°N for AMIP vs ERA-Interim (cyan line) and for 20CRv2 vs ERA-Interim (red line). Excluding the high latitudes where both AMIP and 20CRv2 have known large biases, the error in 20CRv2 is smaller than in AMIP (Figure 6h).

The annual cycle of the zonal wind at 10 m in 20CRv2 is comparable to ERA-Interim, both in terms of intensity and seasonal evolution, for the global ocean and also for the two hemispheres averages (Figures 7a,c). In AMIP both intensities and seasonal evolution differ from ERA-Interim (Figures 7a,c, cyan line). In particular, in the global ocean average the zonal wind at 10 m is overestimated (more negative) in boreal winter (Figure 7a). Comparing the two hemispheres, the bias is larger in the north and the wind is overestimated in boreal winter but underestimated in boreal summer (Figure 7b). Conversely, in the Southern Hemisphere the differences are smaller, still the wind is underestimated compared to both ERA-Interim and 20CRv2 (Figure 7c). In terms of spatial RMSE, it is evident how the errors in AMIP are much larger than in 20CRv2 (Figures 7d,e), with maxima in the extra-tropics and mostly in the western boundaries of the oceans (Figure 7d). In 20CRv2 the differences are less than 1 m/s in both the tropics and extra-tropics (not shown).

Considering the meridional wind component, the biases are generally smaller than for the zonal wind in both

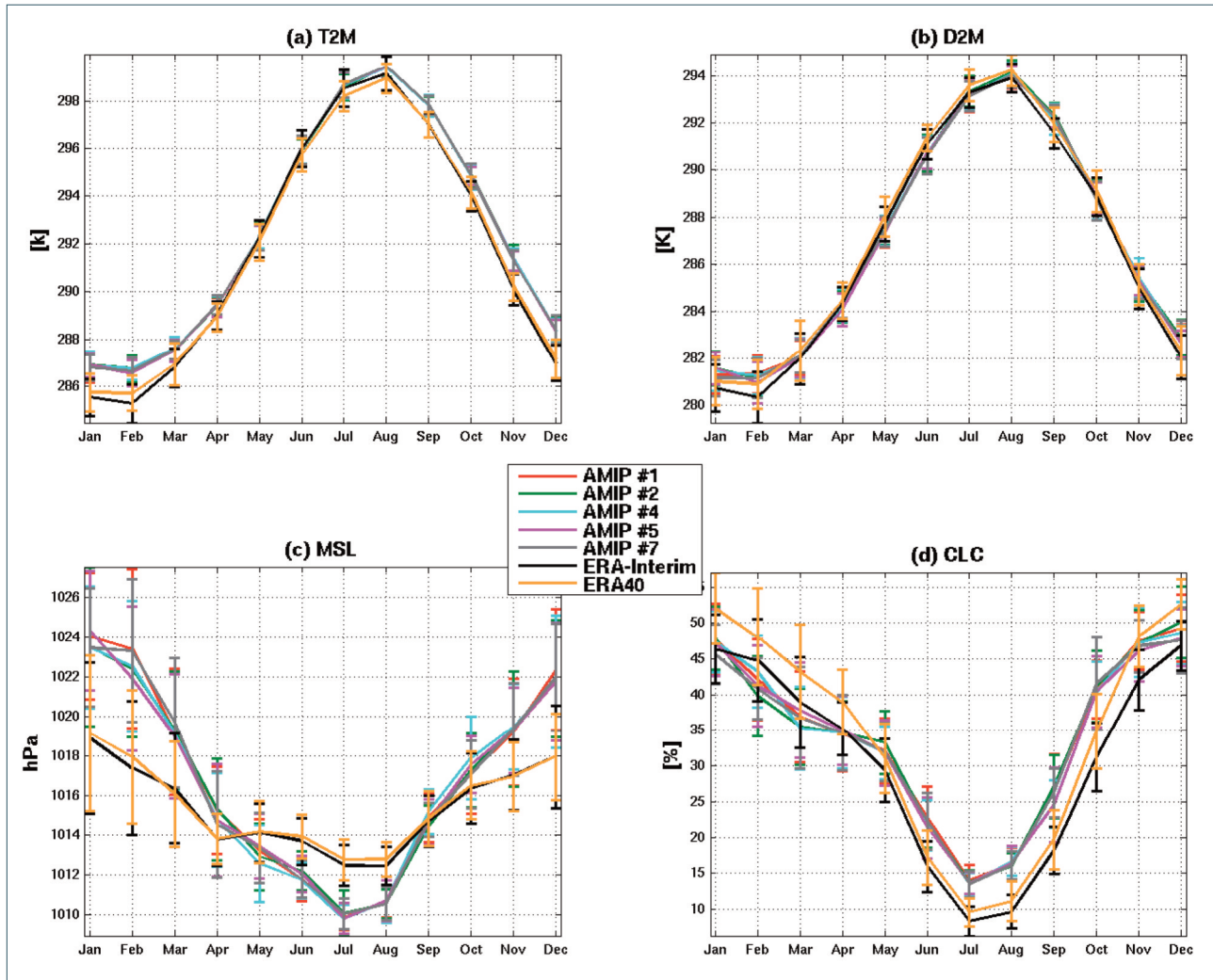


FIGURE 1. Annual cycle of (a) temperature at 2 m (T2M, K), (b) dew point temperature at 2 m (D2M, K), (c) mean sea level pressure (MSL, hPa) and (d) total cloud cover (CLC, %) averaged in the Mediterranean basin for ERA-Interim (black line) and ERA40 (yellow line) reanalyses and for the AMIP members (other colored lines). Climatologies are computed over the common period between the three datasets, 1979-2001. The vertical bars represent the standard deviation with respect to the climatology.

AMIP and 20CRv2 (Figures 8a,c), although AMIP has the largest bias, mostly in the Southern Hemisphere winter (Figure 8c), where it is overestimated. In the spatial pattern RMSE values indicate that AMIP has more regions with large errors, while 20CRv2 have the largest values in intensity but localized in very few areas close to the coasts (Figures 8d,e). As for temperature, Figure 7f and Figure 8f show squared differences of monthly mean wind at 10 m (zonal and meridional, respectively) averaged in the global ocean for AMIP and 20CRv2 vs ERA-Interim (cyan and red line, respectively). In both cases the error is almost constant in time but it is much reduced in 20CRv2 compared to AMIP (Figures 7f,8f).

The annual cycle of downward shortwave radiation shows that the values averaged over the global ocean in AMIP are underestimated compared to ERA-Interim, while in 20CRv2 they are slightly overestimated (Figure 9a). The

largest differences occur in boreal summer (Figures 9b,c) and have a maximum in the Northern Hemisphere. In AMIP the bias is negative almost everywhere except for the eastern boundaries of the ocean (not shown) and the largest RMSE values are in the tropics (Figure 9d). The negative bias indicates that less shortwave radiation reaches the surface, and it is likely that the reason is an excess of low clouds in the tropics (not shown). Conversely, in 20CRv2 the bias is mostly positive (not shown) and RMSE is larger along the western coasts of the continents (Figure 9e).

Similarly, the annual cycle of downward longwave radiation shows the largest RMSE in boreal summer in the Northern Hemisphere in AMIP (Figure 9g). The flux in 20CRv2 has values close to ERA-Interim both in terms of intensity and of seasonal distribution (Figures 9f,g,h red line). Considering the spatial pattern, AMIP has an over-

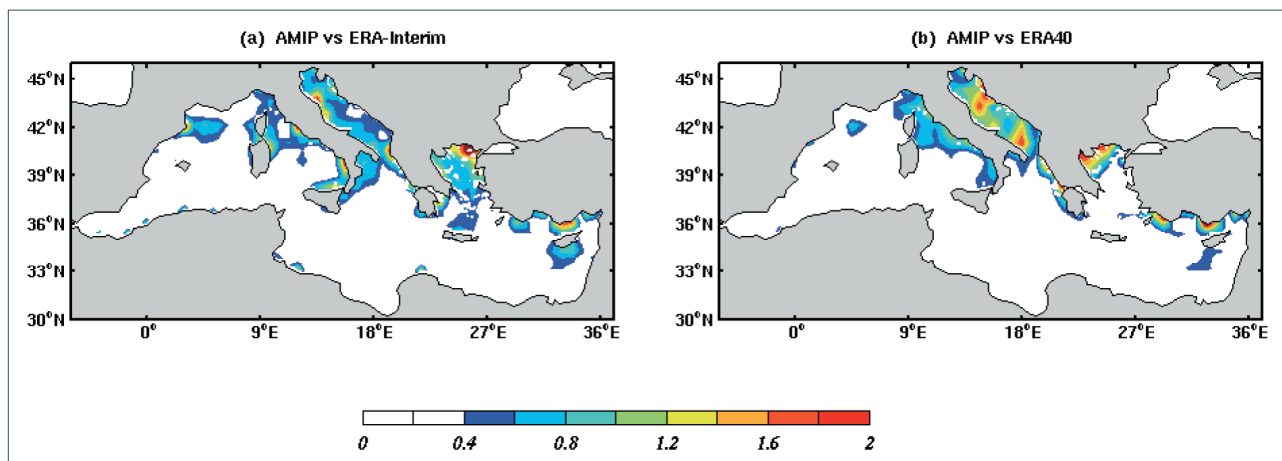


FIGURE 2. Annual mean RMSE of temperature at 2 m of AMIP ensemble mean vs (a) ERA-Interim and (b) ERA40. Climatologies are computed over the common period between the three datasets, 1979-2001.

all positive bias (not shown) with the largest RMSE in the tropics (Figure 9i) and a negative bias mostly in the

Southern Hemisphere in the middle latitudes (not shown). Conversely, the RMSE is generally smaller in 20CRv2 (Fig-

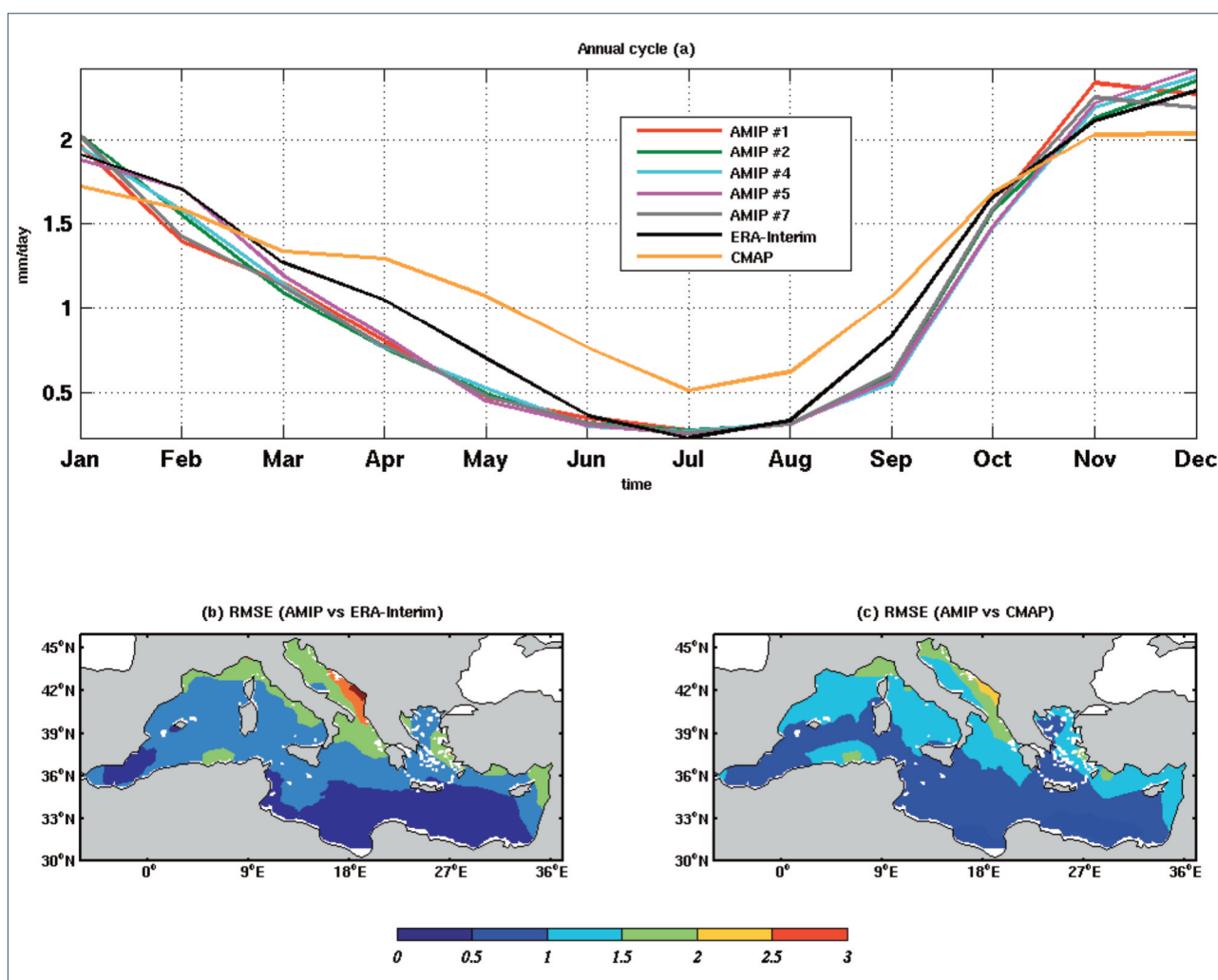


FIGURE 3. (a) Annual cycle of precipitation (mm/d) averaged in the Mediterranean basin for ERA-Interim reanalysis (black line), CMAP data (orange line) and the AMIP members (other colored lines). Climatologies are computed over the common period between the three datasets, 1979-2010. Maps are for annual mean RMSE of precipitation of AMIP (ensemble mean) vs (b) ERA-Interim and (c) CMAP.

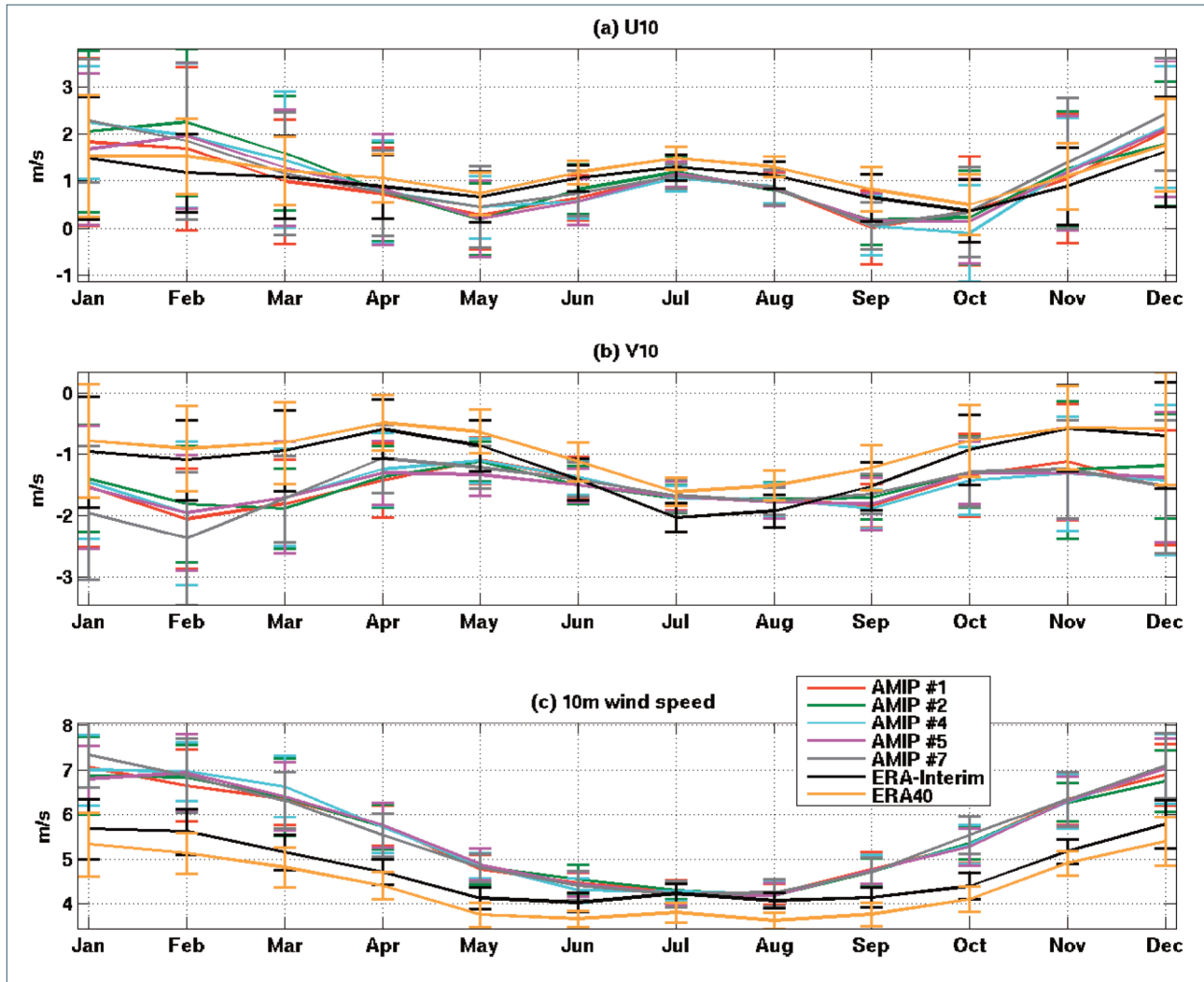


FIGURE 4. Annual cycle of (a) zonal wind (m/s) at 10 m, (b) meridional wind (m/s) at 10 m and (c) 10 m wind speed (m/s) averaged over the Mediterranean basin for ERA40 (yellow line), ERA-Interim (black line) reanalyses and for the AMIP experiments (other colored lines). Climatologies are computed over the common period between the three datasets, 1979-2001. The vertical bars represent the standard deviation with respect to the climatology.

ure 9j) but with some maxima located in the polar regions and along the western coasts of the continents (Figure 9j).

In the south-east Pacific region, off-the coasts of Peru and Chile the westerly large-scale circulation flow interacts with the Andes producing a persistent presence of stratocumulus deck on the Pacific Ocean cooling the SST and stimulating upwelling of ocean currents [Wood et al., 2011]. There the AMIP experiments have large errors mostly in terms of radiation (Figure 9) because these coupled processes between ocean and atmospheric dynamics driven by persistent cloudiness are not represented.

The annual cycle of the corrected ERA-Interim (ERA-Interim) precipitation is shown in Figures 10a,c, together with the same variables from 20CRv2 and AMIP experiments. The annual cycle indicates that 20CRv2 largely overestimates the precipitation averaged over the global ocean, and the bias is comparably large in both hemispheres (Figures 10a,c). In AMIP the bias in terms

of global averages is smaller, but in boreal summer there is more precipitation than observed (Figure 10a). In terms of the spatial pattern, the largest differences are found in the tropics (Figures 10f,g). Both AMIP and 20CRv2 have a negative bias along the western boundaries of the ocean in the Northern Hemisphere (Figure 10d, e). Comparing the maps of annual mean differences, it is clear that both AMIP experiments and 20CRv2 have limitations in terms of total precipitation. In the case of the AMIP experiments the main reason is associated with the well-known deficiencies of models in representing convective processes in the tropics together with the lack, in this type of experiment, of appropriate air-sea feedbacks [Kirtman and Vecchi, 2011]. Monthly mean squared differences in precipitation averaged in the global ocean are generally larger in 20CRv2 than in AMIP (Figure 10h).

When the comparison between AMIP and 20CRv2 of

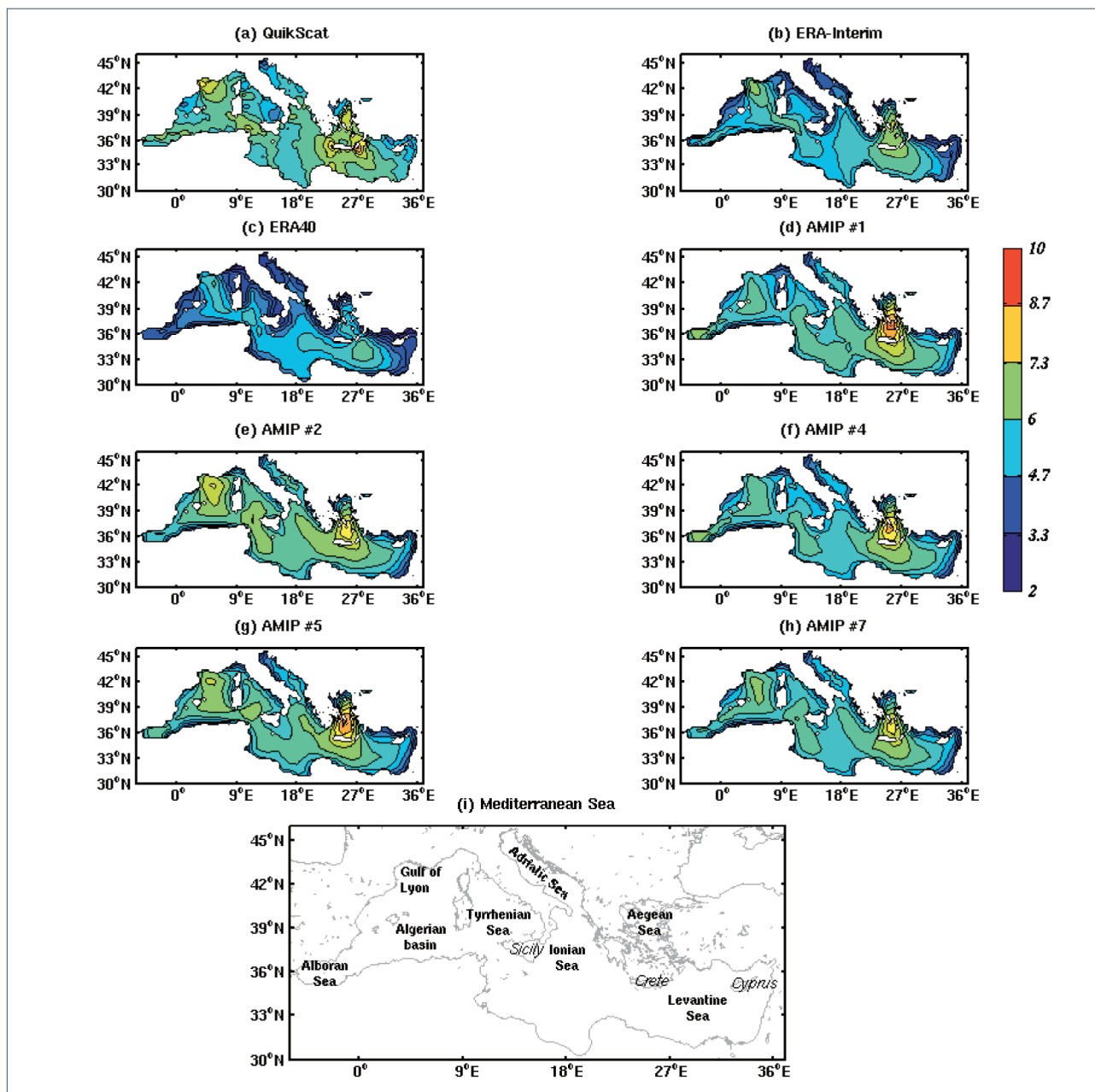


FIGURE 5. Annual mean 10 m wind speed (m/s) for (a) QuikSCAT data, (b) ERA-Interim, (c) ERA40 and (d-h) AMIP experiments. Climatologies are computed over the common period between the datasets, 2000-2003. Panel (i) shows some details of the geography of the Mediterranean Sea.

temperature at 2 m is applied to the longer period (1901-2010), both the annual cycle and its spatial pattern reflect the differences discussed for the shorter period: AMIP is generally warmer than 20CRv2 except in the polar regions where the latter is much warmer (Figure 11a). Apart from the poles, the other largest RMSE in the annual mean are close to the eastern coasts of the Northern Hemisphere continents (Figure 11b). The timeseries of the squared differences averaged from 60°S to 60°N over the ocean, thus excluding the high latitudes, tend to reduce toward the end of the record (Figure 11c). Differences for the other variables in the longer time record are similar to those described for the shorter period (not shown).

3.3 INTERANNUAL VARIABILITY AND TRENDS

To compare the interannual variability as reproduced in the different datasets over both Mediterranean Sea and global ocean, Table 2 and 3 contain standard deviation values and correlation coefficients for temperature, winds and precipitation. The standard deviation values have been computed for the monthly mean anomalies (thus removing the seasonal cycle) averaged over the global ocean and the Mediterranean Sea. For T2M and V10 the values are comparable among the three data sets in the regions considered, while for U10 and PRECIP the values in AMIP are much smaller (i.e. almost halved) than in ERA-Interim, indicating a weaker variability

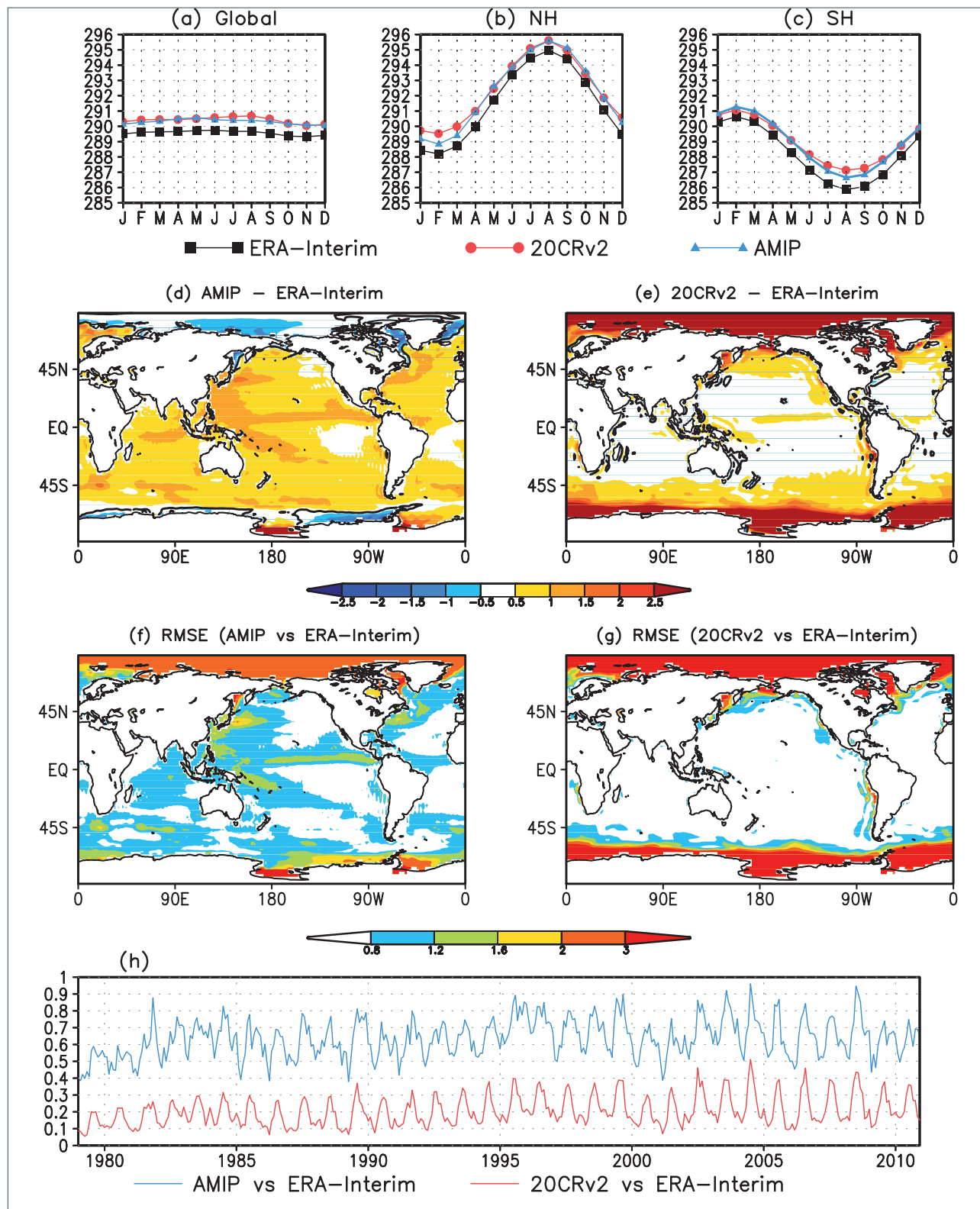


FIGURE 6. Annual cycle of temperature (K) at 2 m (T2M) averaged over (a) the global ocean, (b) the Northern and (c) the Southern Hemisphere oceans (defined as averages from the Equator to the poles). Annual mean T2M in terms of (d, e) differences from ERA-Interim and (f, g) RMSE vs ERA-Interim for AMIP and 20CRv2, respectively. The climatology is computed for the period 1979-2010. (h) Monthly mean squared differences T2M for AMIP and 20CRv2 vs ERA-Interim (cyan and red line, respectively), averaged from 60°S to 60°N (high latitudes are excluded as highly biased).

they are weaker in boreal summer (Figure 12b).

Figure 13 shows the annual mean temperature at 2

m averaged over the global ocean (GLOB) and the Mediterranean Sea (MED). The time series are shown for

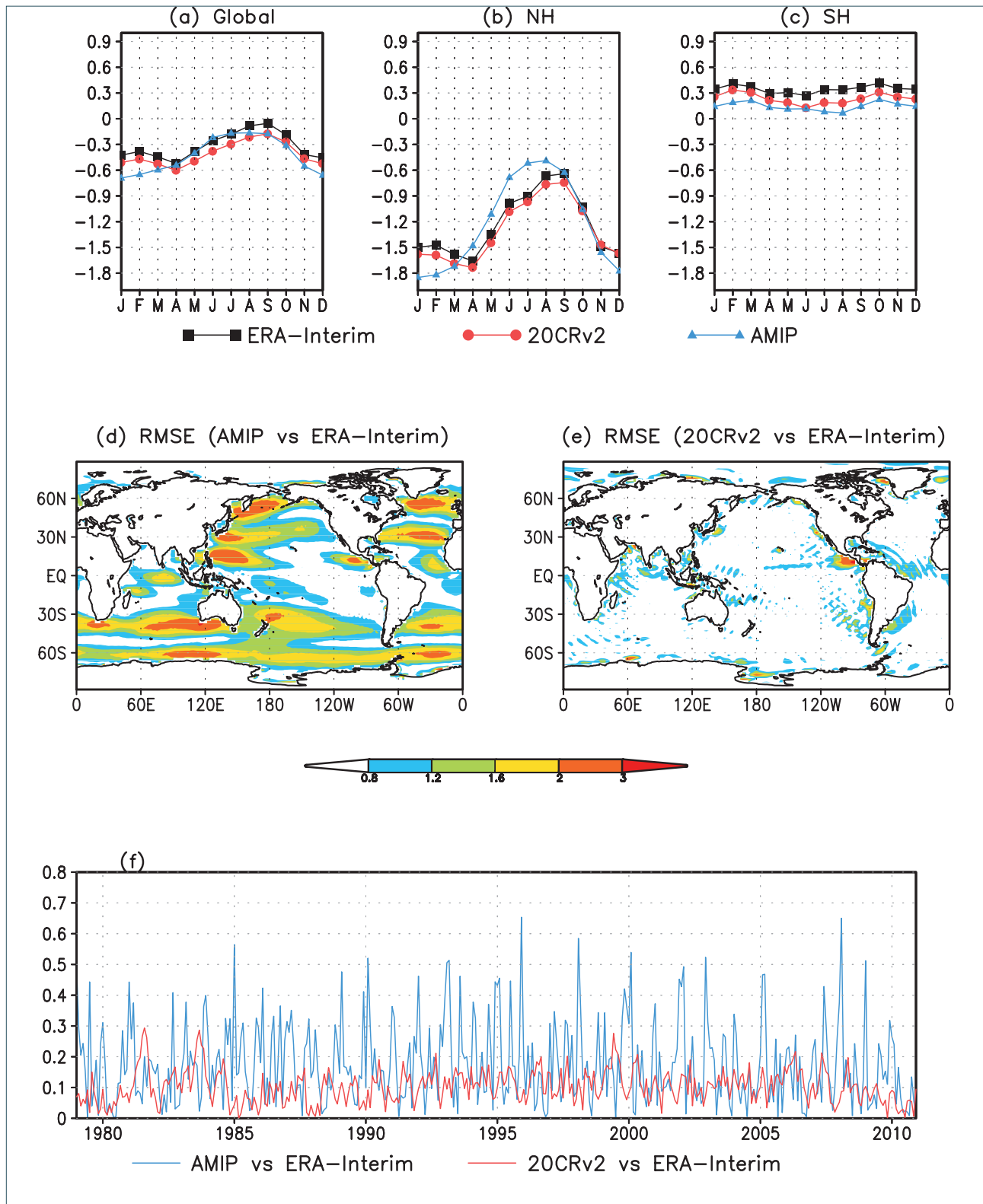


FIGURE 7. Annual cycle of zonal wind (m/s) at 10 m (U10) averaged over (a) the global ocean, (b) the Northern and (c) the Southern Hemisphere oceans (defined as averages from the Equator to the poles). (d,e) Annual mean U10 in terms of RMSE vs ERA-Interim for AMIP and 20CRv2, respectively. The climatology is computed for the period 1979-2010. (f) Monthly mean squared differences of globally averaged U10 (ocean points only) for AMIP and 20CRv2 vs ERA-Interim (cyan and red line, respectively).

ERA-Interim (black line) and 20CRv2 (red line) reanalyses, and for AMIP experiments (cyan line). Both

20CRv2 and AMIP tend to overestimate the temperature close to the surface, as discussed also above in terms of

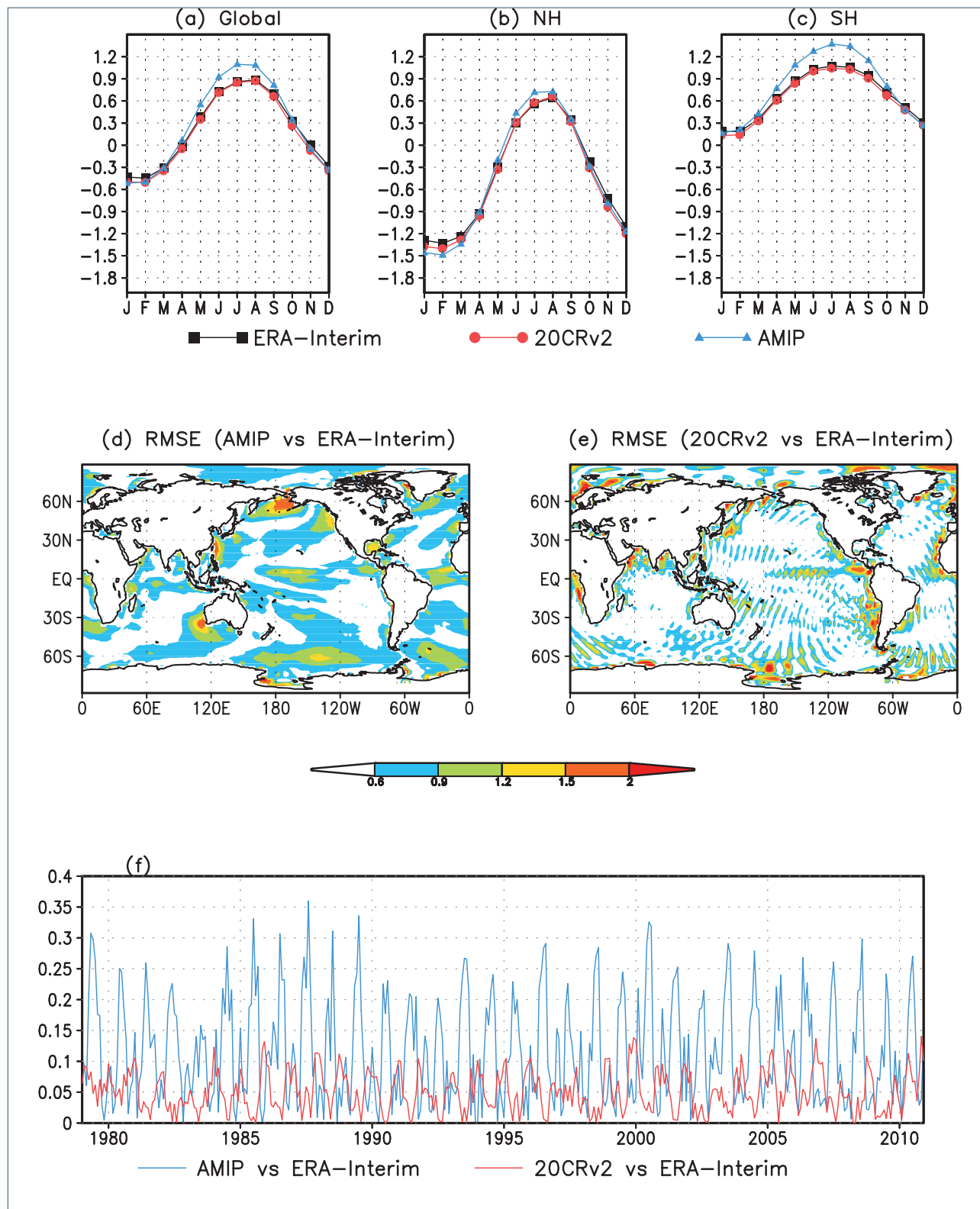


FIGURE 8. Same as Figure 7 but for meridional wind (m/s) at 10 m (V10).

climatologies, but in both datasets, the value of the linear trend for the last decades of the century (i.e. 1979–2010) is realistic when compared with ERA-Interim (Table 4). In fact, over the global ocean the trend in ERA-Interim is about $0.13^\circ\text{C}/\text{decade}$ in agreement with ob-

servational datasets [Foster and Rahmstorf, 2011] and it is 0.13 and $0.14^\circ\text{C}/\text{decade}$ in 20CRv2 and AMIP, respectively (Table 4). When considering the whole century (i.e. 1901–2010) the values in 20CRv2 reanalysis and AMIP experiments are comparable and consistent, with

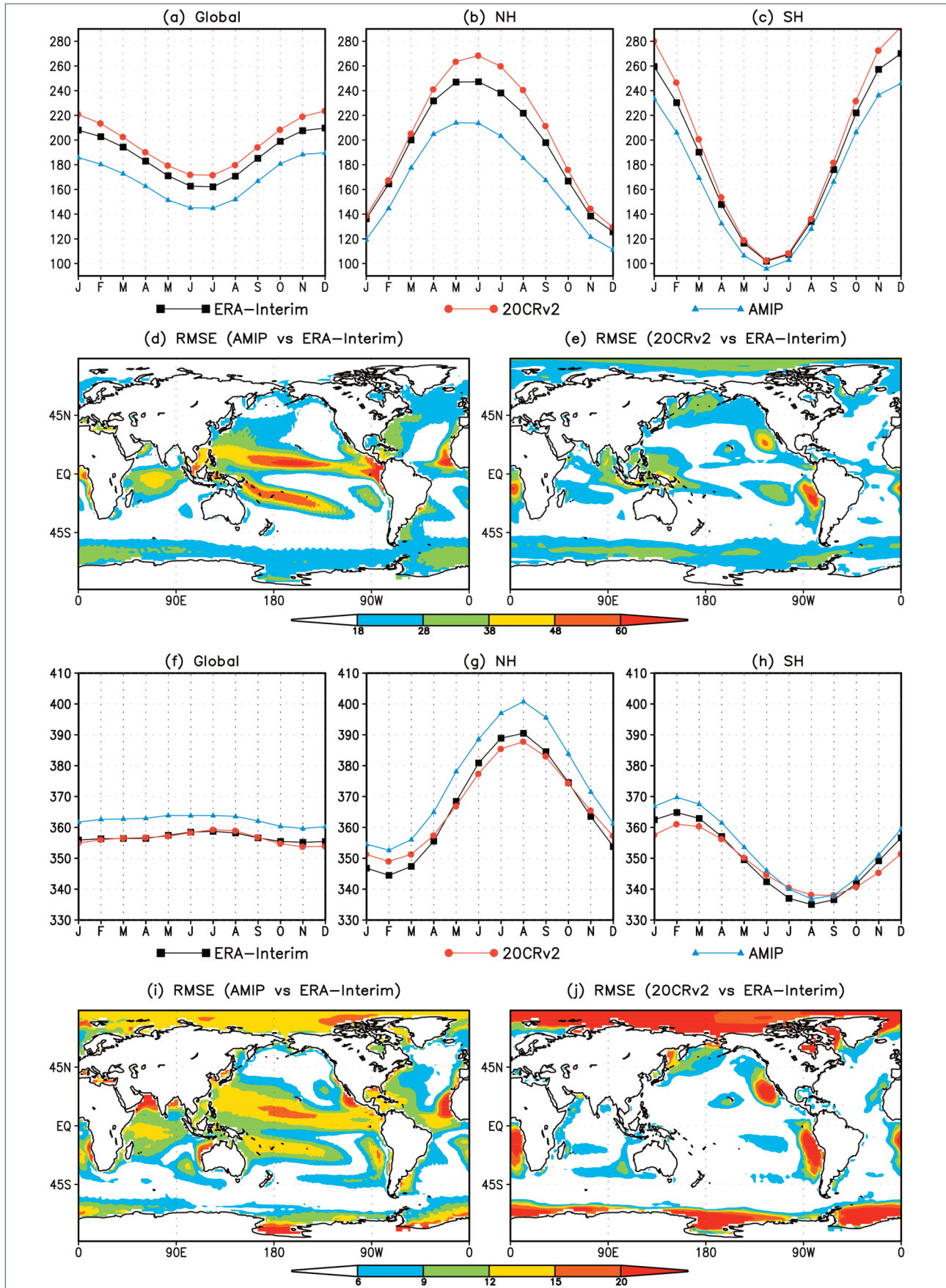


FIGURE 9. Annual cycle of downward shortwave radiation (W/m^2 , SWRD) averaged over (a) the global ocean, (b) the Northern and (c) the Southern Hemisphere oceans (defined as averages from the Equator to the poles). (d,e) Annual mean RMSE of AMIP and 20CRv2 vs ERA-Interim, respectively. (f-h) same as (ac) and (i-j) same as (d-e) but for downward longwave radiation (W/m^2 , LWRD). For both variables, the climatology is computed for the period 1979-2010.

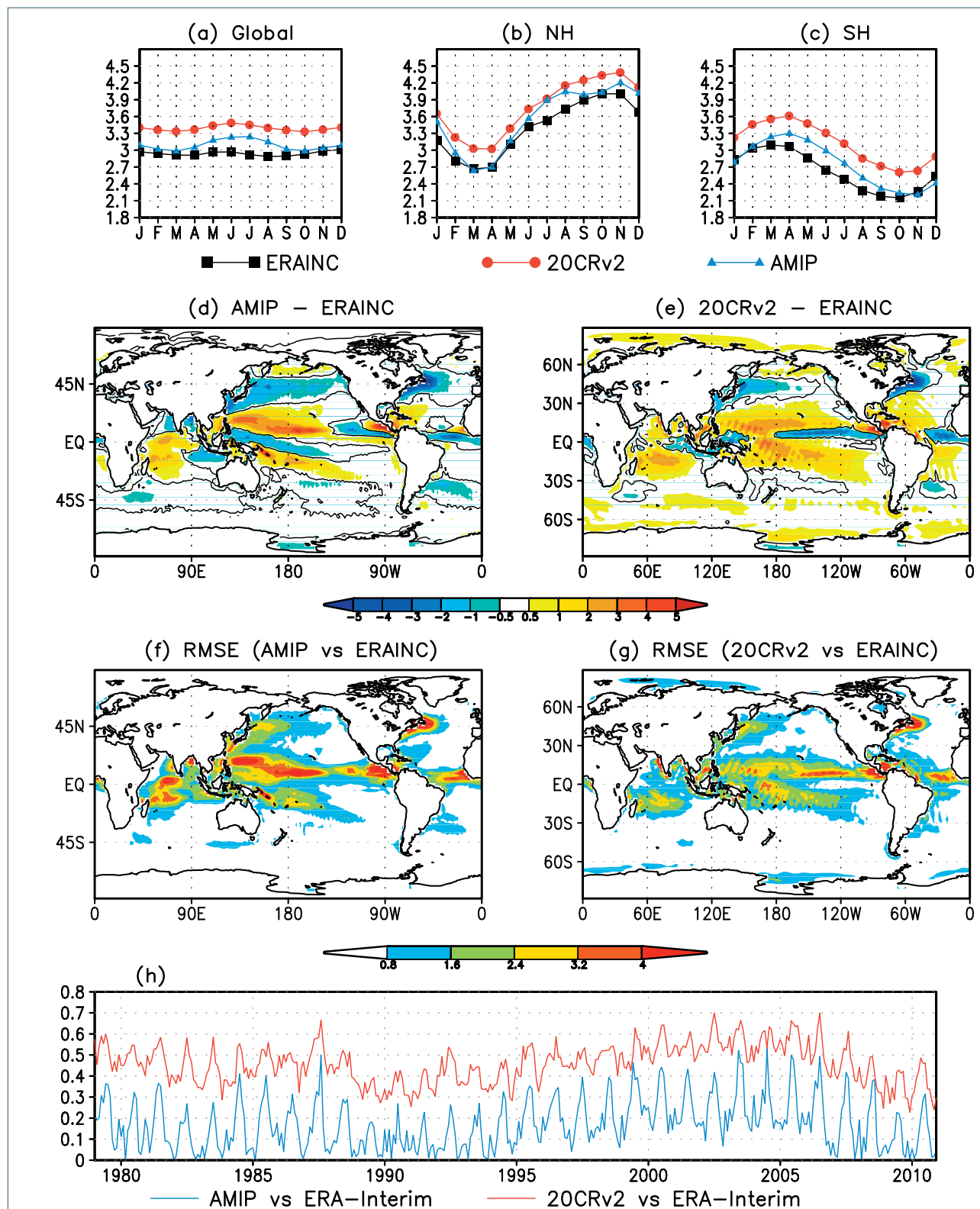


FIGURE 10. Annual cycle of precipitation (mm/d) averaged over (a) global ocean, (b) Northern and (c) Southern Hemisphere oceans. Annual mean PRECIP in terms of (d,e) differences and (f,g) RMSE vs ERA-Interim corrected dataset (ERA-Interim) for AMIP and 20CRv2, respectively. The climatology is computed for the period 1979-2010. (h) Monthly mean squared differences of globally averaged PRECIP for AMIP and 20CRv2 vs ERA-Interim (cyan and red line, respectively).

the trend over the global ocean equals to 0.09 °C/decade in 20CRv2 and to 0.08 °C/decade in AMIP (Table 4).

Despite in the AMIP experiments the transient atmo-

spheric GHG contribution is not directly included in the atmosphere, the trends in temperature close to the surface are reproduced, confirming our hypothesis that the

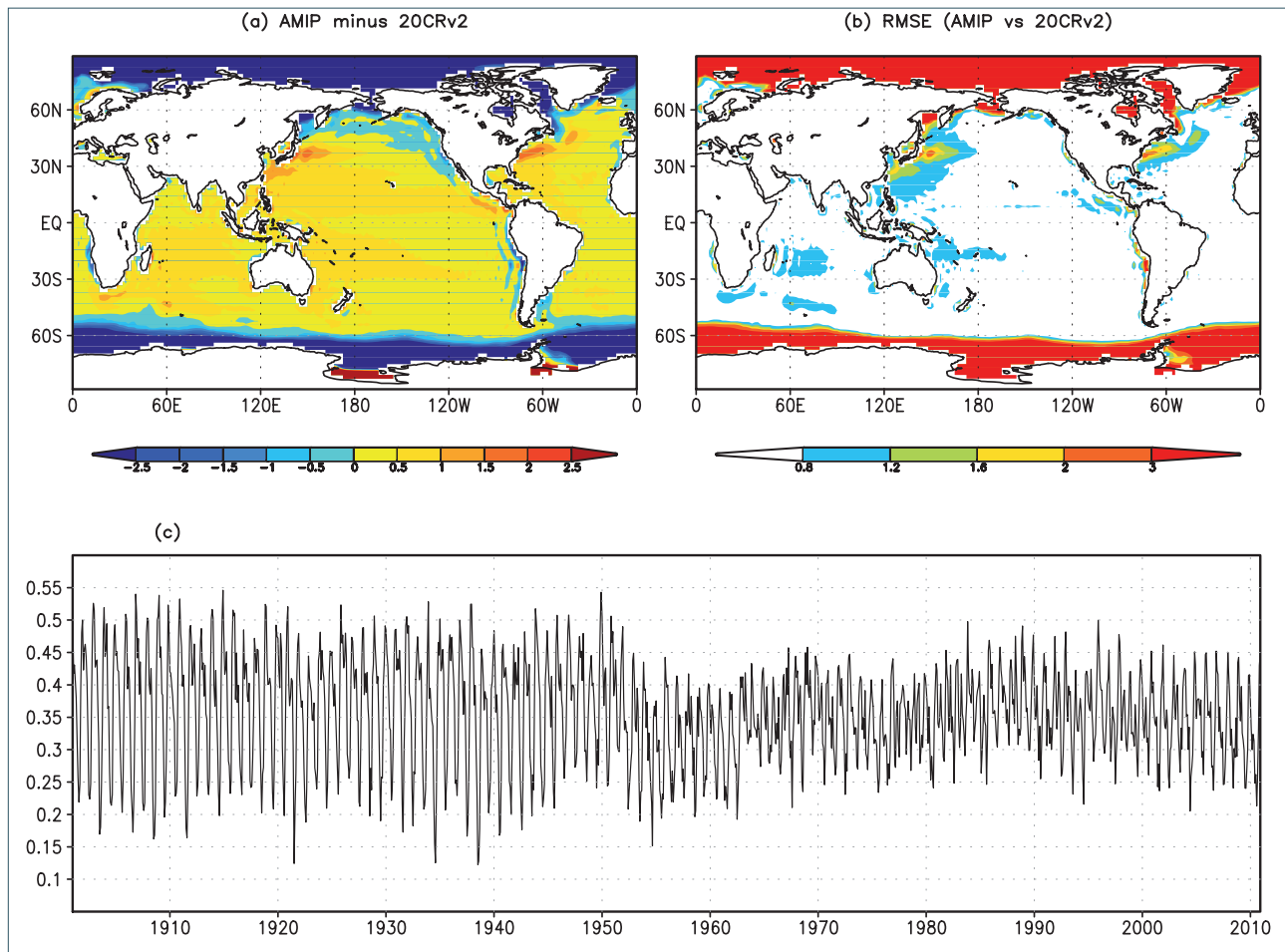


FIGURE 11. (a) Annual mean difference and (b) RMSE of T2M in AMIP vs 20CRv2. The climatology is computed for the period 1901–2010. (c) Monthly mean squared differences of T2M in AMIP vs 20CRv2 averaged from 60°S to 60°N.

SST variability is more important for the ocean model and the data assimilation system than the GHG one is, at least over the ocean. Recently, He and Soden [2016] reinforced and motivated the use of AMIP experiments for simulating anthropogenic changes when resulting from an SST prescribed change, despite the lack of constraints for energetically consistent surface fluxes.

In the case of the zonal wind at 10 m the variability in 20CRv2 is much closer to the ERA-Interim than it is in AMIP (not shown). Considering the discussion in previous sections these results are perfectly in line suggesting that the biases in the ECHAM4 atmospheric model influence the performance in reproducing the surface zonal mean wind and its variability. Rather the assimilation of the sole SLP in 20CRv2 is enough to reproduce the zonal wind either in the mean and in terms of variability. For the trends as reported in Table 4, in the last decades of the 20th century the values are very small (i.e. for the global ocean $-0.03 \text{ ms}^{-1}/\text{decade}$ in ERA-Interim and in 20CRv2, $-0.02 \text{ ms}^{-1}/\text{decade}$ in AMIP). Also considering the whole century, the values for AMIP are smaller than for the 20CRv2 reanalysis (Table 4).

4. CONCLUSIONS AND DISCUSSION

An ensemble of AMIP-type experiments (AMIP) produced with an atmospheric general circulation model prescribed with observed SST and sea-ice concentrations is compared to available atmospheric reanalysis products to evaluate it as atmospheric forcing for ocean data assimilation systems designed for the production of oceanic reanalyses for the whole 20th century. The comparison is divided into an evaluation for the Mediterranean Sea and for the global ocean.

Over the Mediterranean Sea, AMIP members are compared with ERA-Interim and ERA40 reanalyses. The results shown indicate that over the Mediterranean basin AMIP shows a realistic good performance of temperature at 2 m (including dew point temperature), despite some systematic biases in the mean sea level pressure field and in the total cloud cover. In terms of temperature at 2m and precipitation RMSE, the largest differences from ERA40 and ERA-Interim reanalyses values are found in the Adriatic Sea and in the north-eastern side of the basin.

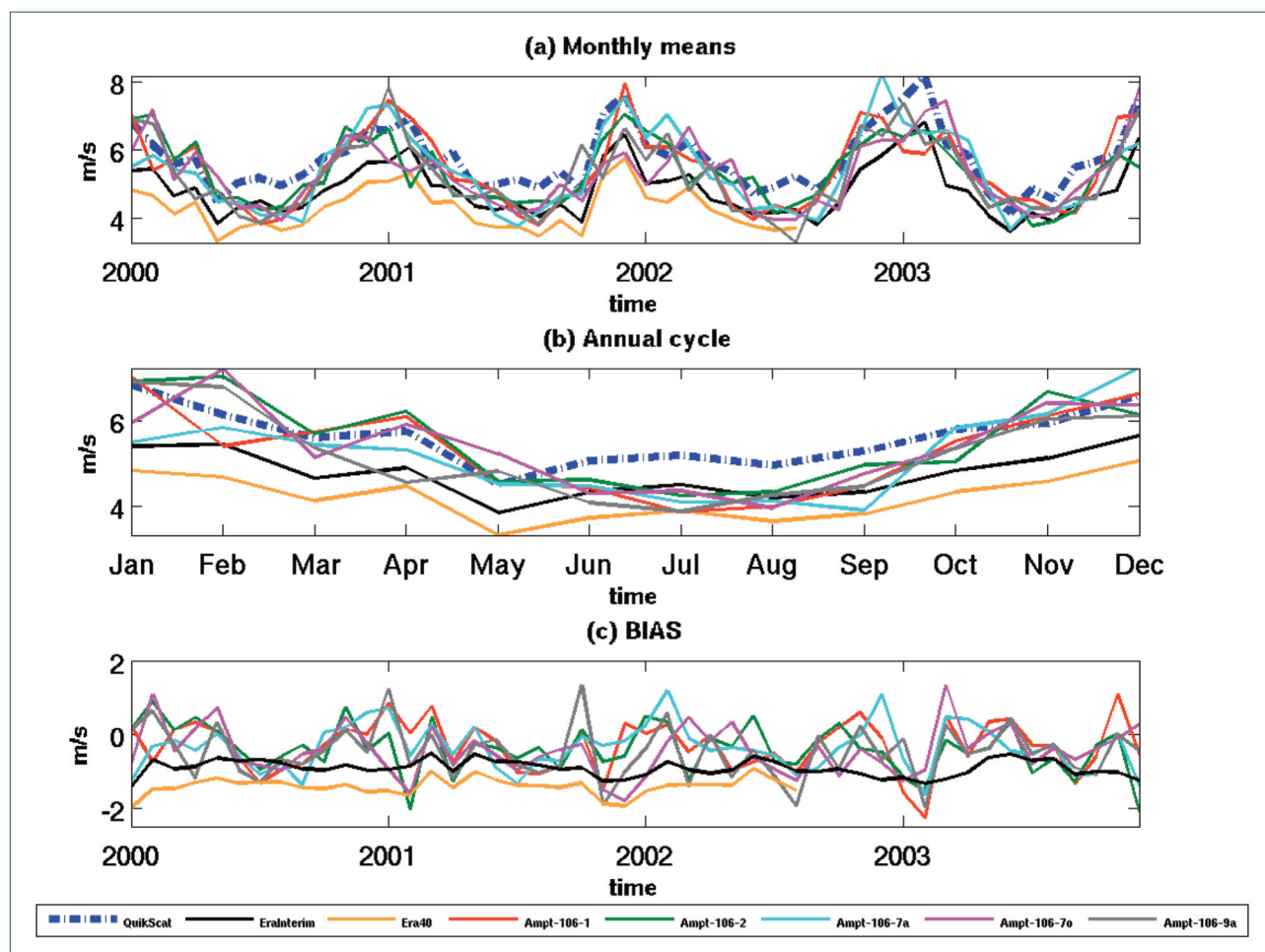


FIGURE 12. 10 m wind speed (m/s) averaged over the Mediterranean basin for the period 2000-2003 in terms of (a) monthly means and (b) annual cycle for QuikSCAT data (blue dashed line), ERA40 (yellow line) and ERA-Interim (black line) reanalyses and for the AMIP experiments (other colored lines). (c) Bias (i.e. difference) of monthly mean wind vs QuikSCAT.

The analysis of the surface winds revealed a surprising good performance both in terms of annual cycle and spatial patterns, specifically when compared with an available short record of satellite data (QuikSCAT). It is likely that the high resolution of the AMIP experiments

as well the potential role of SST forcing in shaping surface wind structures, made them the most suitable candidate to be used as atmospheric forcing for the production of long oceanic reanalyses in the Mediterranean Sea. In a preliminary assessment, the ocean reanalysis

	T2M °C/decade	ERA-Interim	20CRv2 vs	AMIP
1979-2010	GLOB	0.13	0.13	0.14
	MED	0.35	0.27	0.22
1901-2010	GLOB		0.09	0.08
	MED		0.05	0.06
	U10 ms ⁻¹ /decade	ERA-Interim	20CRv2 vs	AMIP
1979-2010	GLOB	-0.03	-0.03	-0.02
	MED	-0.02	-0.05	-0.05
1979-2010	GLOB		0.011	-0.005
	MED		-0.01	-0.01

TABLE 4. Linear trends of annual mean temperature at 2 m (T2M, °C/decade) and zonal wind at 10 m (U10, ms⁻¹/decade) in ERA-Interim, 20CRv2 and AMIP for the 1979-2010 decades and in AMIP and 20CRv2 for the whole century (1901-2010). The trends are computed over the global ocean (GLOB) and the Mediterranean Sea (MED, 6°W-37°E, 30°-46°N).

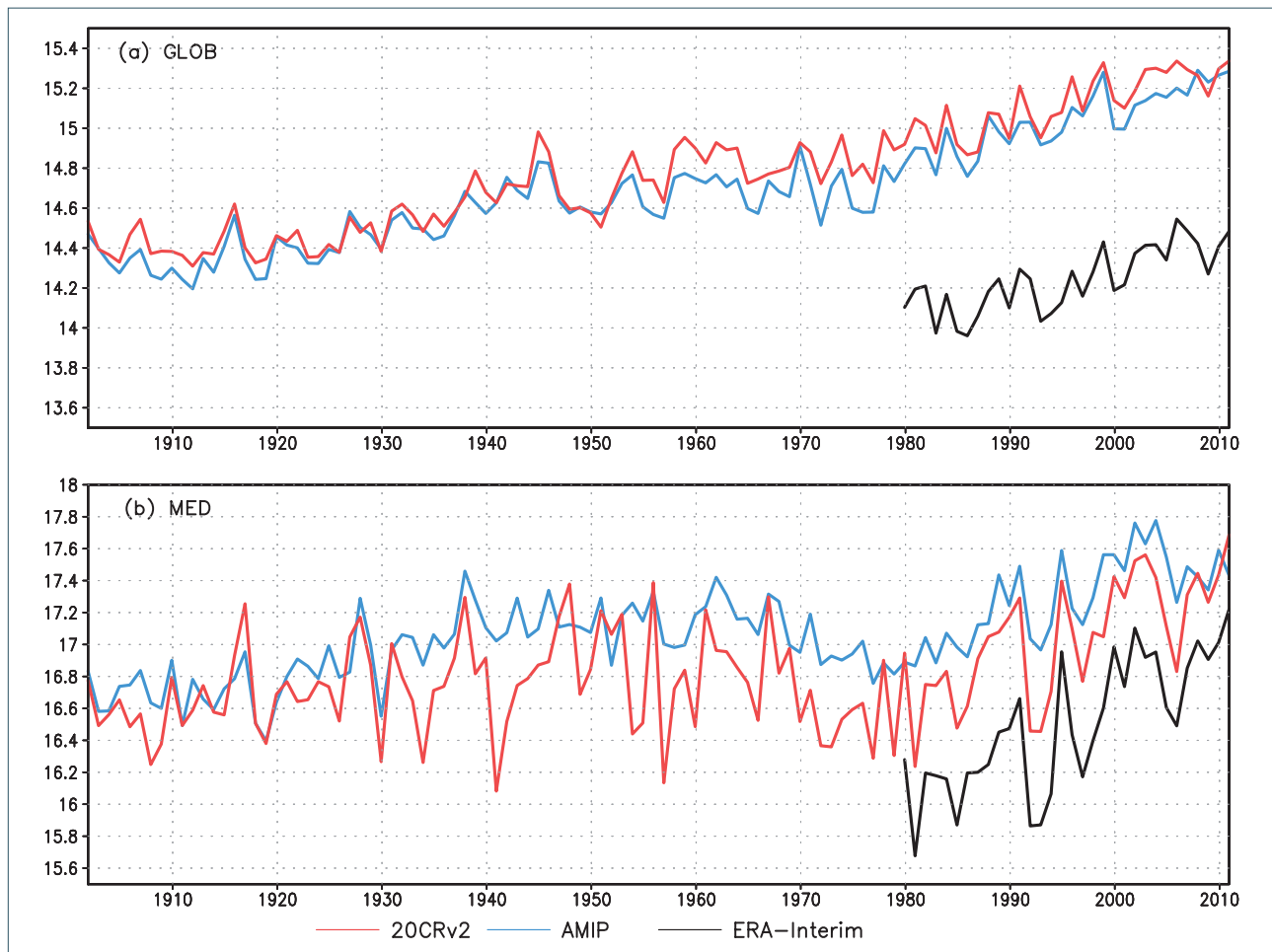


FIGURE 13. Annual mean temperature at 2 m (T2M, K) averaged over (a) global ocean (GLOB) and (b) Mediterranean Sea (MED) for 20CRv2 (red line), AMIP (cyan line) and ERA-Interim (black line) from 1901 to 2010.

forced with AMIP [Fратиanni et al., 2015] is compared with another ocean reanalysis forced with atmospheric forcing from ERA-Interim, and the results indicate that the two reanalyses products are of comparable quality. A detailed work on the overall performance and quality of the new ocean reanalysis in the Mediterranean Sea using AMIP atmospheric fields will follow.

Over the global ocean a comparison is made between AMIP (in terms of ensemble mean), 20CRv2 and ERA-Interim reanalyses. Here ERA-Interim is the reference for the evaluation of the performance of the other two datasets. The main conclusions from this comparison indicate that in terms of annual cycle 20CRv2 is closer to ERA-Interim for meridional wind at 10 m, SWRD and LWRD, but the AMIP ensemble mean is more realistic for the precipitation. They are similar in terms of zonal wind at 10 m. When analyzing the spatial patterns and associated RMS errors, 20CRv2 is found to have more realistic patterns than AMIP in the tropics for temperature at 2 m, meridional and zonal wind at 10 m and downward radiative fluxes. However, 20CRv2 has large biases at high latitudes:

for example, AMIP is more realistic in the polar region in terms of temperature and LWRD, and is more realistic in the mid-latitudes in terms of SWRD. For precipitation both 20CRv2 and AMIP have large biases in the tropics, and both have dry biases in the northwest Pacific and northwest Atlantic sectors.

Combining these results and mostly considering the larger biases found in the spatial patterns in AMIP, 20CRv2 remains a better choice as atmospheric forcing for the global ocean. However, the spectral signature in the wind fields, as well as the warm biases in polar regions, appear two non-negligible weaknesses of the 20CRv2 dataset for ocean reanalysis applications. This justifies the adoption of high-latitude atmospheric forcing bias-correction procedures as those described by Yang et al. [2017] for the production of historical reanalyses. Moreover, the proliferation of century long atmospheric and Earth's system reanalyses [e.g. CERA-20C Laloyaux et al., 2018], will allow to have a better insight on the relative merits of historical atmospheric reanalyses and quantifying the underlying uncertainty.

At interannual timescale AMIP has weaker variability than ERA-Interim in terms of zonal wind at 10 m and precipitation. For precipitation averaged over the global ocean, the correlation coefficient of monthly mean anomalies (AMIP vs ERA-Interim) is the smallest. Conversely, 20CRv2 has standard deviation values of monthly mean anomalies comparable to ERA-Interim and correlation coefficients realistically high and statistically significant for all the variables considered.

In our AMIP experiments the atmospheric GHGs are constant but the SST prescribed from the observations contains the signature of time-varying concentrations of atmospheric gases. In fact, the comparison of linear trends in the last decades between the three datasets indicates that the values found for the temperature at 2 m are comparable and consistent in the global ocean, as well as in the Mediterranean Sea. This result suggests that the SST variability is more important than that from GHGs alone, at least over the ocean. For zonal winds, the intensity of the trends in AMIP is generally underestimated though very small. AMIP has important shortcoming in the simulation of the mean zonal wind and of its variability, except for the Northern Hemisphere high-latitudes and the Mediterranean region. The comparison of the trends during the whole century between AMIP and 20CRv2 shows values highly consistent in terms of temperature and zonal wind.

In our exercise, atmospheric forcing from AMIP experiments have been evaluated as the optimal choice for the Mediterranean Sea oceanic reanalysis because of their relatively high resolution and the realistic representation of surface winds in the region, probably driven by prescribed SST forcing. Our objective here is not to promote AMIP atmospheric forcing as better than atmospheric reanalyses, rather we intend to show that for specific applications and considering their intrinsic limits they could be of some use. At the time of our analysis the ECMWF centennial atmospheric reanalysis (ERA20C) was not yet distributed, at present or in the coming future it could be interesting and useful repeating our exercise considering the 20th century atmospheric reanalyses now available.

Acknowledgements. We are grateful to the editor and the anonymous reviewers for their comments, as they largely helped improving the manuscript. The financial support of the Italian Ministry of Education, University and Research, and Ministry for Environment, Land and Sea through the project GEMINA is gratefully acknowledged. The analysis for the Mediterranean Sea was supported by the NextData project, funded by the Italian Ministry of Education, University and Research, and by MyOcean Follow On project, funded by Horizon2020 (EU Research and Innovation Programme 2014-2020).

REFERENCES

- Adler R.F, Huffman G.J, Chang A., Ferraro R., Xie P., Janowiak J., Rudolf B., Schneider U., Curtis S., Bolvin D., Gruber A., Susskind J., Arkin P. (2003). The Version 2 Global Precipitation Climatology Project (GPCP) Monthly Precipitation Analysis (1979-Present). *J Hydrometeor* 4: 1147-1167.
- Alessandri A., Borrelli A., Masina S., Carril A.F, Di Pietro P., Cherchi A., Gualdi S., Navarra A. (2010). The INGV-CMCC seasonal prediction system: improved ocean initial conditions. *Mon Wea Rev* 138(7): 2930-2952.
- Alexander M.A., Blade' I., Newman M., Lanzante J.R., Lau N.C., Scott J.D. (2002). The atmospheric bridge: The influence of ENSO teleconnections on air-sea interaction over the global oceans. *J Clim* 15: 2205-2231.
- Allen R.J., Norris J.R., Kovilakam M. (2014). Influence of anthropogenic aerosols and the Pacific Decadal Oscillation on tropical belt width. *Nature Geoscience* 7: 270-274.
- Beljaars A.C.M., Bechtold P., Kohler M., Orr A., Tompkins A.M. (2006). Developments in model physics after ERA40. In *Proceedings of the ECMWF/GEO Workshop on atmospheric reanalysis*, Reading, UK, 1922 June, 8190.
- Balmaseda M.A., Fujii Y., Alves O., Lee T., Rienecker M., Rosati T., Stammer D., Xue Y., Freeland H., McPhaden M.J., Goddard L., Coelho C. (2009). Role of ocean observing system in an end-to-end seasonal forecasting system. *Proceedings of OceanObs'09. Sustained observations and information for society*. Hall J, Harrison DE, Stammer D Eds ESA Publication WPP-306, Venice, Italy 21-25 September 2009.
- Bellucci A., Gualdi S., Masina S., Storto A., Scocimarro E., Cagnazzo C., Fogli P.G., Manzini E., Navarra A. (2013). Decadal climate predictions with a coupled OAGCM initialized with oceanic reanalysis. *Clim Dyn* 40: 1483-1497.
- Bentamy A., Croize-Fillon D. (2012). Gridded surface wind fields from Metop/ASCAT measurements. *Int J Rem Sensing* 33(6): 1729-1754.
- Brodeau L., Barnier B., Treguier A.M., Penduff T., Gulev S. (2010). An ERA40-based atmospheric forcing for global ocean circulation models. *Oc Model* 31: 88-104.
- Cessi P., Pinardi N., Lyubartsev V. (2014). Energetics of semi-enclosed basins with two-layer flows at the strait. *J Phys Oceanogr* 44: 967-979 doi: <http://dx.doi.org/10.1175/JPO-D-13-0129.1>.

- Chaudhuri A.H., Ponte R.M., Forget G., Heimbach P. (2013). A comparison of atmospheric reanalysis surface products over the ocean and implications for uncertainties in air-sea boundary forcing. *J Clim* 26: 153-170.
- Cherchi A., Kucharski F., Colleoni F. (2018). Remote SST forcing on Indian summer monsoon extreme years in AGCM experiments. *Int J Clim* 38: e160-e177 doi: 10.1002/joc.5360.
- Cherchi A., Carril A., Menendez C., Zamboni L. (2014). La Plata basin precipitation variability 542 in spring: role of remote SST forcing as simulated by GCM experiments. *Clim Dyn* 42: 219-236.
- Cherchi A., Navarra A. (2013). Influence of ENSO and of the Indian Ocean Dipole on the Indian summer monsoon variability. *Clim Dyn* 41: 81-103 DOI: 10.1007/s00382-012-1602-y.
- Compo G.P., Whitaker J.S., Sardeshmukh P.D., Matsui N., Allan R.J., Yin X., Gleason B.E., Vose R.S., Rutledge G., Bessemoulin P., Bronnimann S., Brunet M., Crouthamel R.I., Grant A.N., Groisman P.Y., Jones P.D., Kruk M., Kruger A.C., Marshall G.J., Maugeri M., Mok H.Y., Nordli O., Ross T.F., Trigo R.M., Wang X.L., Woodruff S.D., Worley S.J. (2011). The Twentieth Century Reanalysis Project. *Quart J Roy Meteor Soc* 137: 1-28 DOI: 10.1002/qj.776.
- Dee D.P., Uppala S.M. (2009). Variational bias correction of satellite radiance data in the ERA-Interim reanalysis. *Q J R Meteorol Soc* 135: 1830-1841.
- Dee D.P., Uppala S.M., Simmons A.J., Berrisford P., Poli P., Kobayashi S., Andrae U., Balmaseda M.A., Balsamo G., Bauer P., Bechtold P., Beljaars A.C.M., van de Berg L., Bidlot J., Bormann N., Delsol C., Dragani R., Fuentes M., Geer A.J., Haimberger L., Healy S.B., Hersbach H., Hólm E.V., Isaksen L., Kållberg P., Köhler M., Matricardi M., McNally A.P., Monge-Sanz B.M., Morcrette J.J., Park B.K., Peubey C., de Rosnay P., Tavolato C., Thépaut J.N., Vitart F. (2011). The ERA-Interim re-analysis: configuration and performance of the data assimilation system. *Quart J Roy Meteor Soc* 137: 553-597.
- Demirov E., Pinardi N. (2002). The simulation of the Mediterranean Sea circulation from 1979 to 1993. Part I: the interannual variability. *J Mar Syst* 33-34: 23-50.
- Dussin R., Barnier B. (2013). The Making of DFS 5.1. Drakkar Reports. 40 pp <http://www.drakkar-ocean.eu/publications/reports/dfs5-1-report>.
- Foster G., Rahmstorf S. (2011). Global temperature evolution 1979-2010. *Env Res Lett* 6: 044022 doi: 10.1088/1748-9326/6/4/044022.
- Fratianni C., Simoncelli S., Pinardi N., Cherchi A., Grandi A., Dobricic S. (2015). Mediterranean RR 1955-2015 (version 1) [dataset]. Copernicus Monitoring Environment Marine Service (CMEMS).
- Gates W.L. (1992). AMIP: the Atmospheric Model Inter-comparison Project. *Bull Am Meteorol Soc* 73: 1962-1970.
- Grassi B., Redaelli G., Canziani P.O., Visconti G. (2012). Effects of the PDO phase on the tropical belt width. *J Climate* 25: 3282-3290.
- He J., Soden B.J. (2016). Does the lack of coupling is SST-forced atmosphere-only models limit their usefulness for climate change studies? *J Climate* 29: 4317-435.
- Hilburn K., Wentz F. (2008). Inter-calibrated passive microwave rain products from the Unified Microwave Ocean Retrieval Algorithm (UMORA). *J Appl Meteorol Clim* 47: 778-794.
- Hersbach H., Peubey C., Simmons A., Berrisford P., Poli P., Dee D. (2015). ERA-20CM: a twentieth century atmospheric model ensemble. *Quart J Roy Meteor Soc* 141: 2350-2375 doi: 10.1002/qj.2528.
- Janowiak J.E., Bauer P., Wang W., Arkin P., Gottschalck J. (2010). An evaluation of precipitation forecasts from operational models and reanalyses including precipitation variations associated with MJO activity. *Mon Wea Rev* 138: 4542-4560.
- Kalnay E., Kanamitsu M., Kistler R., Collins W., Deaven D., Gandin L., Iredell M., Saha S., White G., Woollen J., Zhu Y., Chelliah M., Ebisusaki W., Higgins W., Janowiak J., Mo K.C., Ropelewski C., Wang J., Leetmaa A., Reynolds R., Jenne R., Joseph D. (1996). The NCEP/NCAR 40-years reanalysis project. *Bull Am Meteorol Soc* 77(3): 437-471.
- Kent E.C., Fangohr S., Berry D.I. (2013). A comparative assessment of monthly mean wind speed products over the global ocean. *Int J Climatol* 33: 2520-2541.
- Kirtman B., Vecchi G.A. (2011). Why climate modelers should worry about atmospheric and oceanic weather. In: Chang CP, Ding Y, Lau NC, Jonhson RH, Wang B, Yasunari T (Eds) "The global monsoon system: research and forecast", 2nd Edition, World Scientific Series on Asia-Pacific Weather and Climate, 511-524.
- Korres G., Pinardi N., Lascaratos A. (2000). The ocean response to low frequency interannual atmospheric variability in the Mediterranean Sea. Part I: sensitivity experiments and energy analysis. *J Climate* 13: 732-745 doi: 10.1175/1520-0442(2000)013<0705:TORTLF>2.0.CO₂;
- Krishnamurthy V., Kirtman B.P. (2003). Variability of the

- Indian Ocean: relation to monsoon and ENSO. *Q J Roy Meteor Soc* 129: 1623-1646.
- Laloyaux P., de Boisseson E., Balmaseda M., Bidlot J.R., Broennimann S., Buizza R. et al. (2018). CERA20C: A coupled reanalysis of the twentieth century. *Journal of Advances in Modeling Earth Systems* 10 <https://doi.org/10.1029/2018MS001273>.
- Large W.G., Yeager S.G. (2009). The global climatology of an interannually varying air-sea flux data set. *Clim Dyn* 33: 341-364 doi:10.1007/s00382-008-0441-3.
- Large W.G., Yeager S.G. (2004). Diurnal to decadal global forcing for ocean and sea-ice models: the data sets and flux climatologies. NCAR Tech Rep NCAR/TN-460+STR, 105 pp.
- Lau N.C., Nath M.J. (1994). A modelling study of the relative roles of tropical and extra-tropical SST anomalies in the variability of the global atmosphere-ocean system. *J Clim* 7: 1184-1207.
- Mantua N.J., Hare S.R., Zhang Y., Wallace J.M., Francis R.C. (1997). A Pacific interdecadal climate oscillation with impacts on salmon production. *Bull Am Meteor Soc* 78: 1069-1079.
- Masina S., A. Storto, N. Ferry, M. Valdivieso, K. Haines, M. Balmaseda, H. Zuo, M. 606 Drevillon, L. Parent, (2017). An ensemble of eddy-permitting global ocean reanalyses from the MyOcean project. *Clim Dyn*, 49 (3): 813-841.
- Masina S., Di Pietro P., Storto A., Navarra A. (2011). Global ocean re-analyses for climate applications. *Dyn Atm Oc* 52: 341-366.
- Milliff R.F., Bonazzi A., Wikle C.K., Pinardi N., Berliner L.M. (2011). Ocean ensemble forecasting. Part I: Ensemble Mediterranean winds from a Bayesian hierarchical model. *Quart J Roy Meteor Soc* 137: 858-878 doi: 10.1002/qj767.
- Myers P.G., Haines K., Josey S. (1998). On the importance of the choice of wind stress forcing to the modelling of the Mediterranean Sea circulation. *J Geophys Res* 103: 15,729-15,749.
- Oddo P., Adani M., Pinardi N., Fratianni C., Tonani M., Pettenuzzo D (2009). A nested Atlantic-Mediterranean Sea general circulation model for operational forecasting. *Ocean Sci* 5: 461-473.
- Onogi K., Koide H., Sakamoto M., Kobayashi S., Tsutsui J., Hatsushika H., Matsumoto T., Yamazaki N., Kamahori H., Takahashi K., Kato K., Oyama R., Ose T., Kadokura S., Wada K. (2005). JRA-25: Japanese 25-year reanalysis project - progress and status. *Quart J Roy Meteor Soc* 131: 3259-3268.
- Palmer T.N. (1993). Extended-range atmospheric prediction and the Lorenz model. *Bull Am Meteor Soc* 74: 49-65.
- Pettenuzzo D., Large W.G., Pinardi N. (2010). On the corrections of ERA-40 surface flux products consistent with the Mediterranean heat and water budgets and the connection between basin surface total heat flux and NAO. *J Geophys Res Oc* 115 C06022 doi: 10.1029/2009JC005631.
- Pinardi N., Zavatarelli M., Adani M., Coppini G., Fratianni C., Oddo P., Simoncelli S., Tonani M., Lyubartsev V., Dobricic S. and Bonaduce A. (2015). Mediterranean Sea large-scale low-frequency ocean variability and water mass formation rates from 1987 to 2007: a retrospective analysis. *Progress in Oceanography*, 132, pp.318-332.
- Pohlmann H., Smith D.M., Balmaseda M.A., Keenlyside N.S., Masina S., Matei D., Muller W.A., Rogel P. (2013). Predictability of the mid-latitude Atlantic meridional overturning circulation in a multi-model system. *Clim Dyn* 41: 775-785 doi: 10.1007/s00382-013-1663-6.
- Poli P., Hersbach H., Tan D., Dee D., Thpaut J.N., Simmons A., Peubey C., Laloyaux P., Komori T., Berrisford P., Dragani R., Trmolet Y., Holm E., Bonavita M., Isaksen L., Fisher M. (2013). The data assimilation system and initial performance evaluation of the ECMWF pilot reanalysis of the 20th century assimilating surface observations only (ERA-20C). ERA Report Series 14, ECMWF, 59pp <http://old.ecmwf.int/publications/library/do/references/show?id=90833>.
- Rayner N.A., Parker D.E., Horton E.B., Folland C.K., Alexander L.V., Rowell D.P., Kent E.C., Kaplan A. (2003). Global analyses of sea surface temperature, sea ice, and night marine air temperature since the late nineteenth century. *J Geophys Res* 108(D14) 4407 DOI: 10.1029/2002JD002670.
- Roeckner, E., K. Arpe, L. Bengtsson, M. Christoph, M. Claussen, L. Du'menil, M. Esch, M. Giorgetta, U. Schlese and U. Schulzweida, 1996. The Atmospheric general circulation Model ECHAM4: Model description and simulation of present-day climate: Max-Planck Institut fu'r Meteorologie, Report no. 218, Hamburg, 86 pp.
- Rowntree P.R. (1972). The influence of the tropical east Pacific Ocean temperature on the atmosphere. *Q J Roy Meteor Soc* 98: 290-321.
- Rowntree P.R. (1976). Tropical forcing of atmospheric motions in a numerical model. *Q J Roy Meteor Soc* 102: 583-605.
- Simoncelli S., Pinardi N., Oddo P., Mariano A.J., Monatnari G., Rinaldi A., Deserti M. (2011). Coastal rapid environmental assessment in the Northern Adriatic

- Sea. Dyn Atm Oc 52 (1-2) 250-283 doi:10.1016/j.dynatmoce.2011.04.004.
- Simoncelli S., Masina S., Axell L., Liu Y., Salon S., Cos-sarini G., Bertino L., Xie J., Samuelsen A., Levier B., et al. (2016). MyOcean regional reanalyses: overview of reanalyses systems and main results. *Mercator Ocean J.* 54. Special Issue on Main Outcomes of the MyOcean2 and MyOcean Follow-on projects. Available from: <https://www.mercator-ocean.fr/wp-content/uploads/2016/03/JournalMO-54.pdf>.
- Simoncelli S., Bonaduce A., Tonani M. (2015). Quality information document for Mediterranean Sea physical re-analysis product. MyOcean FollowOn Project H2020-Adhoc-2014-20 50 <http://marine.copernicus.edu/documents/QUID/CMEMS-MED-QUID-006-004.pdf>.
- Simoncelli S., Pinardi N. (2018). Water mass formation processes in the Mediterranean Sea over the past 30 years. Section 3.4 in von Schuckmann et al. (2018) CopernicusMarine Service Ocean State Report, Issue 2, *Journal of Operational Oceanography*, 11:sup1, s1s142, DOI: 10.1080/1755876X.2018.1489208.
- Stern W., Miyakoda K. (1995). Feasibility of seasonal forecasts inferred from multiple GCM simulations. *J Clim* 8: 1071-1085.
- Stickler A., Bronnimann S., Valente M.A., Bethke J., Sterin A., Jourdain S., Roucaute E., Vasquez M.V., Reyes D.A., Allan R., Dee D. (2014). ERA-CLIM: Historical surface and upper-air data for future reanalyses. *Bull Am Meteor Soc* 95: 1419-1430 doi: 10.1175/BAMS-D-13-00147.1.
- Storto A., Masina S., Navarra A. (2016). Evaluation of the CMCC eddy-permitting global ocean physical reanalysis system (C-GLORS, 1982-2012) and its assimilation components. *Quart J Roy Meteor Soc* 142: 738-758 doi: 10.1002/qj.2673.
- Storto A., Russo I., Masina S. (2012). Interannual response of global ocean hindcasts to a satellite-based correction of precipitation fluxes. *Ocean Sci Discuss* 9: 611-648 doi:10.5194/osd-9-611-2012.
- Tonani M., Teruzzi A., Korres G., Pinardi N., Crise A., Adani M., Oddo P., Dobricic S., Fratianni C., Drudi M., Salon S., Grandi A., Girardi G., Lyubartsev V., Marino S. (2011). The Mediterranean Monitoring and Forecasting Centre, a component of the MyOcean system. Proceedings of the Sixth International Conference on EuroGOOS, 4-6 October 2011, Sopot, Poland. Dahlin H, Fleming NC, Petersson SE eds, Eurogoos Publication no. 30, ISBN 978-91-974828-9-9.
- Tonani M., Pinardi N., Adani M., Bonazzi A., Coppini G., De Dominicis M., Dobricic S., Drudi M., Fabbroni N., Fratianni C., Grandi A., Lyubartsev V., Oddo P., Pettenuzzo D., Pistoia J., Pujol I. (2008). The Mediterranean ocean Forecasting system, Coastal to Global Operational Oceanography: Achievements and Challenges. Proceedings of the Fifth International Conference on EuroGOOS, 20-22 May 2008, Exeter, UK. Dahlin H, Bell MJ, Fleming NC, Petersson SE eds, Eurogoos Publication no. 28, ISBN 978-91-974828-6-8.
- Uppala S.M., Kallberg P.W., Simmons A.J., Andrae U., da Costa Bechtold V., Fiorino M., Gibson J.K., Haseler J., Hernandez A., Kelly G.A., Li X., Onogi K., Saarinen S., Sokka N., Allan R.P., Andersson E., Arpe K., Balmaseda M.A., Beljaars A.C.M., van de Berg L., Bidlot J., Bormann N., Caires S., Chellier F., Dethof A., Dragosavac M., Fisher M., Fuentes M., Hagemann S., Holm E., Hoskins B.J., Isaksen I., Janssen P.A.E.M., Jenne R., McNally A.P., Mahfouf J.F., Morcrette J.J., Rayner N.A., Saunders R.W., Simon P., Sterl A., Trenberth K.E., Untch A., Vasiljevic D., Viterbo P., Woollen J. (2005). The ERA-40 re-analysis. *Quart J Roy Meteor Soc* 131: 2961-3012 DOI:10.1256/qj.04.176.15.
- Wood R., Mechoso C.R., Bretherton C.S., Weller R.A., Huebert B., Straneo F., Albrecht B.A., Coe H., Allen G., Vaughan G., Daum P., Fairall C., Chand D., Gallardo Klenner L., Garreaud R., Grados C., Covert D.S., Bates T.S., Krejci R., Russell LM., de Szoeke S, Brewer A., Yuter S.E., Springston S.R., Chaigneau A., Toniazzo T., Minnis P., Palikonda R., Abel S.J., Brown W.O.J., Williams S., Fochesatto J., Brioude J., Bower K.N. (2011). The VAMOS ocean-cloud-atmosphere-land study regional experiment (VOCALS-REx): goals, platforms, and field operations. *Atm Chem Phys* 11: 627-654 doi: 10.5194/acp-11-627-2011.
- Xie P., Arkin P.A. (1997). Global precipitation: A 17-year monthly analysis based on gauge observations, satellite estimates and numerical model outputs. *Bull Am Meteor Soc* 78: 2539-2558.
- Yang C., Giese B. (2013). El Nino Southern Oscillation in an ensemble ocean reanalysis and coupled climate models. *J Geophys Res* 118: 4052-4071 doi: 10.1002/jgrc.20284.
- Yang C., Masina S., Storto A. (2017). Historical ocean reanalyses (1900-2010) using different 702 data assimilation strategies. *Quart J Roy Meteorol Soc* 143: 479-493 doi:10.1002/qj.2936.
- Yang C., Giese B., Wu L. (2014). Ocean dynamics and tropical Pacific climate change in ocean reanaly-

CHERCHI ET AL.

ses and coupled climate models. J Geophys Res
119: 7066-7077 doi: 10.1002/2014JC009979.

***CORRESPONDING AUTHOR:** Annalisa CHERCHI,
Fondazione Centro Euro-Mediterraneo sui Cambiamenti Climatici,
Bologna,
Italy
email: annalisa.cherchi@ingv.it

© 2018 the Istituto Nazionale di Geofisica e Vulcanologia.
All rights reserved.